Received: 1 March 2019 | Revised: 21 June 2019 | Accepted: 21 August 2019

DOI: 10.1002/dep2.92

ORIGINAL RESEARCH ARTICLE

The Depositional Record Open Access
A journal of the International Association of Sedimentologists
WILEY

Sedimentation in a synclinal shallow-marine embayment: Coniacian of the North Sudetic Synclinorium, SW Poland

Stanisław Leszczyński[1] | **Wojciech Nemec**[2]

[1]Institute of Geological Sciences, Jagiellonian University, Kraków, Poland

[2]Department of Earth Science, University of Bergen, Bergen, Norway

Correspondence
Wojciech Nemec, Department of Earth Science, University of Bergen, 5007 Bergen, Norway.
Email: wojtek.nemec@uib.no.

Funding information
Project funded from university personal research accounts of the authors.

Abstract

This study is a reconstruction of the Coniacian palaeogeographic and palaeoenvironmental development in the North Sudetic Basin, a synclinal trough within the Late Cretaceous Central European seaway linking the Boreal and Tethyan marine provinces. The basin formed as an early side effect of the Alpine orogeny combined with the mid-Cretaceous eustasy, and crucial stages of its evolution occurred during the Coniacian. The basin in the early Coniacian was a long and narrow shallow-marine embayment with a hypothetical (non-preserved) bayhead strait funnelling tidal currents. Coalescing tidal sand ridges formed a littoral platform that prograded from the bayhead zone along the basin axis, impinged on laterally by the basin-margin shoreface and local river deltas. A mid-Coniacian forced marine regression and closure of the bayhead strait, attributed to the Alpine tectonism combined with eustasy, brought about a dramatic change in the basin, whereby the basin-wide littoral sand platform emerged and turned briefly into a denudated coastal plain. The late Coniacian eustatic marine transgression formed an in-place growing coastal sand barrier at the outer edge of the former littoral platform, sheltering a paralic limno-lagoonal plain with peat-forming mires. The coastal barrier was eventually drowned by the sea and maximum marine flooding occurred, followed by a normal regression recorded as a rapidly upwards-shallowing succession of offshore-transition to fluvio-deltaic deposits. This case study of the sedimentation pattern in an evolving, tectonically controlled marine embayment contributes to the existing facies models for estuarine embayments formed by a passive marine drowning of large fluvial or glacial valleys.

KEYWORDS

Ichnofacies, lithofacies, North Sudetic Basin, paralic plain, shoal-water deltas, shoreface, tidal sand ridges

1 | INTRODUCTION

The vast majority of reported case studies on sedimentation in long and relatively narrow marine embayments are from drowned fluvial or glacial valleys with bayhead river deltas, falling broadly into the category of estuaries (Boyd *et al.*, 1992; Dalrymple *et al.*, 1994, 2006; Perillo, 1995; Dalrymple, 2010; Gilbert *et al.*, 2018). The present case study of the Coniacian in the North Sudetic Synclinorium, SW Poland (Figure 1A), documents a tectonically created

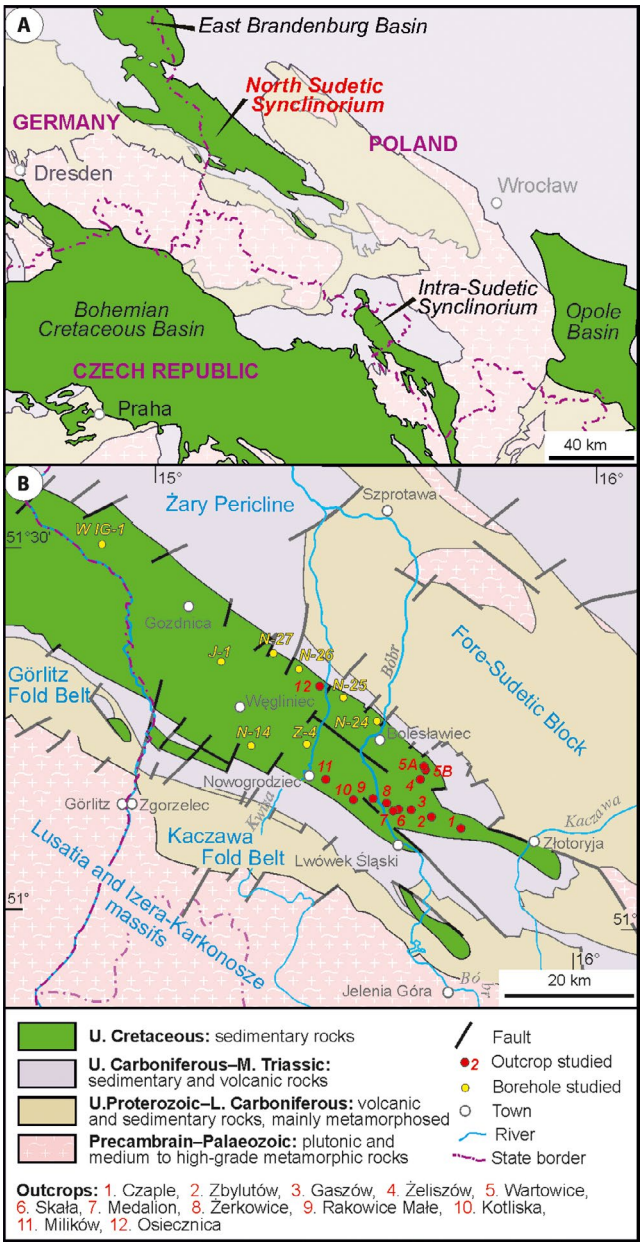

FIGURE 1 (A) Location of the North Sudetic Synclinorium relative to the northern margin of the Bohemian Massif; geological map without the Cenozoic, modified from Pożaryski et al. (1979). (B) Location of the studied outcrops (quarries) and borehole profiles in the North Sudetic Synclinorium; geological map without the Cenozoic, compiled from Pożaryski et al. (1979) and Milewicz (1997). For detailed information on outcrop localities see Table 1

synclinal shallow-marine embayment in which the littoral inner zone initially funnelled tidal currents from a bayhead strait and subsequently—after the strait tectono-eustatic closure—evolved into a paralic coastal plain hosting a mosaic of small rivers, lakes and peat-forming mires.

This study of the sedimentation pattern in a tectonically controlled marine embayment with an initial bayhead strait adds to the estuarine facies models for embayments formed as passively sea-drowned incised valleys (Dalrymple *et al.*, 1992; Dalrymple, 2010). Emphasis is placed on the palaeoenvironmental evolution and dynamic stratigraphy of the inner embayment, reviewing its sedimentary facies assemblages and documenting its responses to a forced regression and a subsequent marine transgression followed by normal regression. At a regional level, the present study is a significant contribution to an understanding of the sedimentary environment and palaeogeographic development in the Late Cretaceous North Sudetic Basin, which was a main component of the Central European seaway linking the Boreal and Tethyan provinces and was eventually inverted by Alpine tectonism into the present-day North Sudetic Synclinorium (Figure 1B).

2 | REGIONAL GEOLOGICAL SETTING

The present-day North Sudetic Synclinorium is a well-preserved axial relic of the Cretaceous North Sudetic Basin—one of the epicontinental shallow-marine basins that formed in the mid-Cretaceous within and around the Bohemian Massif (Figure 1A) as a side effect of the Alpine orogeny. These basins formed at the Central European interface of the Tethyan and Boreal provinces by a regional reactivation of the older, mainly Variscan, fault zones dissecting the Bohemian Massif and its surroundings. The basins were tectonically inverted by regional contraction at the Laramian climax of the orogeny near the end of the Cretaceous. The North Sudetic Basin formed as a southeastern extension of the East Brandenburg Basin (Musstow, 1968; Voigt *et al.*, 2008) and was at least temporarily connected by hypothetical straits with the adjacent Intra-Sudetic Basin and further with the large Bohemian Basin (Figure 1A; Partsch, 1896; Scupin, 1910; Leszczyński, 2018).

The southeast-trending North Sudetic Synclinorium (Figure 1B) is bordered to the northeast by the elevated crystalline Fore-Sudetic Block, devoid of Mesozoic deposits, and by its northwestern envelope known as the Żary Pericline, with a cover of Permian to Middle Triassic deposits. To the southwest, the North Sudetic Synclinorium is bordered by the elevated Görlitz and Kaczawa fold belts (Figure 1B) made of pre-Permian metamorphic rocks (Żelaźniewicz *et al.*, 2011).

3 | BASIN STRATIGRAPHY

The Cretaceous deposits in the North Sudetic Synclinorium overlie a discontinuous succession of Carboniferous to Middle Triassic sedimentary rocks (Figure 1B). These Cenomanian to Santonian deposits are nearly 1,000 m thick (Bossowski *et al.*, 1976; Bossowski, 1991a) and include sandstones, mudstones, claystones and marlstones, with subordinate limestone

TABLE 1 The exact location and stratigraphic position of field outcrops (quarries) investigated in the present study; see basin stratigraphy in Figure 2

No.	Locality name	Outcrop GPS coordinates	Outcrop type	Exposed stratigraphy
1	Czaple (four quarries labelled A–D)	Quarry 1A 51°08′29″N 15°45′36″E	Active quarry at the top of Kopka hill, operated by Gruszecki Ltd.	Sandstones of the Żerkowice Mb. (uppermost Rakowice Wielkie Fm.) exposed in all these quarries. Local relics of the lowermost part of Czerna Fm. preserved in quarry 1B.
		Quarry 1B 51°08′28″N 15°45′40″E	Active quarry at the top of Kopka hill, operated by Kamieniarz Ltd.	
		Quarry 1C 51°08′32″N 15°45′11″E	Abandoned quarry on south-western slope of Kopka hill, owned by Kamieniarz Ltd.	
		Quarry 1D 51°08′41″N 15°44′52″E	Abandoned quarry at the western foot of Kopka hill, owned by Kamieniarz Ltd.	
2	Zbylutów	51°08′57″N 15°39′31″E	Active quarry Zbylutów IV, operated by Kopalnia Piaskowca JAN.	Sandstones of the Żerkowice Mb. (uppermost Rakowice Wielkie Fm.).
3	Gaszów	51°09′32″N 15°37′5″E	Long-abandoned quarry, overgrown by vegetation.	Sandstones of the Żerkowice Mb. (uppermost Rakowice Wielkie Fm.).
4	Żeliszów	51°11′5″N 15°38′54″E	Recently re-activated quarry operated by Kamieniarz Ltd.	Sandstones of the Żerkowice Mb. (uppermost Rakowice Wielkie Fm.).
5	Wartowice	Outcrop A 51°12′45″N 15°39′12″E	Active quarry operated by Hofmann Natursteinwerke Polen GmbH.	Sandstones of the Żerkowice Mb. (uppermost Rakowice Wielkie Fm.) overlain by coal-bearing muddy to sandy deposits of the lowermost Czerna Fm.
		Outcrop B 51°13′06″N 15°38′50″E	Active quarry operated by ATS Stein Ltd.	
6	Skała I	51°09′35″N 15°34′57″E	Active quarry operated by Hofmann Natursteinwerke Polen GmbH.	Sandstones of the Żerkowice Mb. (uppermost Rakowice Wielkie Fm.).
7	Skała II	51°09′30″N 15°34′30″E	Rock tor Medalion.	Sandstones of the Żerkowice Mb. (uppermost Rakowice Wielkie Fm.).
8	Żerkowice	51°09′40″N 15°34′26″E	Active quarry operated by Kopalnie Piaskowca S.A. Bolesławiec.	Sandstones of the Żerkowice Mb. (uppermost Rakowice Wielkie Fm.).
9	Rakowice Małe (Rakowiczki)	51° 9′57″N 15°32′33″E	Recently abandoned quarry owned by Kopalnie Piaskowca S.A. Bolesławiec.	Sandstones of the Żerkowice Mb. (uppermost Rakowice Wielkie Fm.) overlain by lowermost Czerna Fm.
10	Kotliska	51°09′48″N 15°30′51″E	Long-abandoned quarry overgrown by vegetation.	Sandstones of the Żerkowice Mb. (uppermost Rakowice Wielkie Fm.).
11	Milików	51°11′13″N 15°26′18″E	Group of closely spaced, long-abandoned and overgrown quarries.	Sandstones of the Żerkowice Mb. (uppermost Rakowice Wielkie Fm.).
12	Osiecznica	51°19′40″N 15°23′45″E	Active quarry operated by Kopalnia i Zakład Przeróbczy Piasków Szklarskich Ltd.	Sandstones of the top part of Żerkowice Mb. (Rakowice Wielkie Fm.) overlain by lowermost Czerna Fm.

intercalations (Milewicz, 1965, 1997). Outcrops and drilling cores show considerable lateral and vertical variation of these deposits, with siliciclastic sandstone lithosomes dominant to the southeast and pinching out in mudstones and marlstones towards the northwest (Figure 2). Lithostratigraphic interpretation of the sedimentary succession has evolved with time (see review by Milewicz, 1997), with the early German geologists in the region referring to the thick sandstone lithosomes broadly as Quadersandstein (Beyrich, 1849). The existing lithostratigraphy (Figure 2) was proposed by Milewicz (1985), who subdivided the succession into three formations. The marine lower half of the succession—dominated by sandstones to the southeast and by mudstones, marlstones and limestones to the northwest—was labelled as the Rakowice

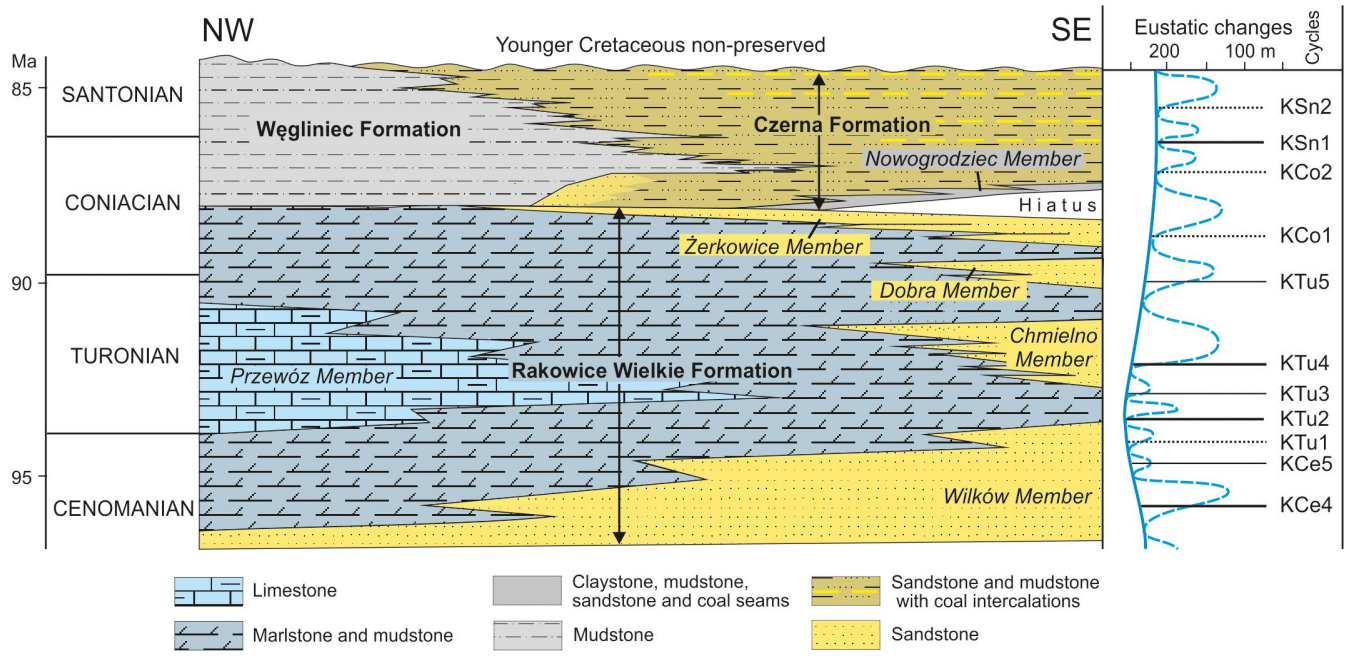

FIGURE 2 The Upper Cretaceous stratigraphy of the North Sudetic Synclinorium, shown in an axial cross-section. Lithostratigraphy is after Milewicz (1997), chronostratigraphy after Walaszczyk (2008) and numerical ages after Cohen et al. (2013); the corresponding eustatic curve is redrawn from Haq (2014)

Wielkie Formation, with its main sandstone lithosomes distinguished as separate members (Figure 2). The upper half of the succession was divided by Milewicz (1985) into two coeval formations, referred to as the Węgliniec Formation and Czerna Formation (Figure 2). The former is marine, composed chiefly of mudstones, whereas the latter to the southeast is paralic, comprising sandstones intercalated with mudstones, claystones and thin coal seams, autochthonous to hypautochthonous (Milewicz, 1965). The mud-dominated limnic lowermost part of the Czerna Formation, rich in coal and 2–50 m thick, was distinguished by Milewicz (1985) as a poorly defined Nowogrodziec Member (Figure 2).

The first biostratigraphic dating of this succession, by Beyrich (1855), suggested a Cenomanian–Senonian age for the deposits. Milewicz (1958) reduced the age of the upper part of the succession to Santonian, and Krutzsch (1966) specified it further as early Santonian. Milewicz (1956, 1979) also postulated a late Coniacian (late Emscherian) hiatus between the Rakowice Wielkie Formation and Czerna Formation in the southeastern part of the North Sudetic Synclinorium, with a decline of this stratigraphic gap towards the northwest (Figure 2).

A more recent biostratigraphic study by Walaszczyk (2008) revised the succession chronostratigraphy. The boundary between the Rakowice Wielkie Formation and the overlying Węgliniec and Czerna formations was assigned to the middle/late Coniacian transition, with the Coniacian/Santonian boundary in the middle of these latter formations and with the hiatus corresponding to the late middle Coniacian (Figure 2). This revised chronostratigraphy is followed in the present paper.

The present study of the Coniacian in the southeastern part of the North Sudetic Synclinorium focusses on what is exposed: the uppermost sandstone member of the Rakowice Wielkie Formation, referred to as the Żerkowice Member by Milewicz (1985) and earlier called the Oberer Quadersandstein (Drescher, 1863; Williger, 1882) and the overlying lower part of the Czerna Formation (Figure 2).

4 | PREVIOUS STUDIES

The Cretaceous deposits of the North Sudetic Synclinorium have been studied since the 19th century and recognized as shallow marine to paralic, based on lithofacies and body fossils (Beyrich, 1849; Drescher, 1863; Williger, 1882; Partsch, 1896; Scupin, 1910). The shallow-marine origin of the succession was confirmed by Milewicz (1958, 1965). The sandstone members of the Rakowice Wielkie Formation (Figure 2) were attributed to a shoreface to foreshore environment, with the mudstones, marlstones and limestones to the northwest representing an offshore environment (Milewicz, 1991, 1998). Bassyouni (1984) suggested a strong influence of tidal currents for the deposition of sandstone lithosomes. A lacustrine environment with peat-forming mires was suggested for the basal Nowogrodziec Member of the Czerna Formation (Figure 2), whereas a mixed brackish and deltaic to alluvial environment was suggested for the overlying

higher part of the formation (Górniak, 1986; Milewicz, 1965, 1991, 1997). These palaeoenvironmental interpretations, although largely intuitive and poorly evidenced by sedimentological data, were broadly confirmed and further elaborated upon by Leszczyński (2010, 2018) based on lithofacies and ichnofauna.

Palaeontological data collected over nearly two centuries have indicated that the Cretaceous sedimentation in the North Sudetic Basin commenced with the worldwide Cenomanian transgression and proceeded until at least the middle Santonian (Beyrich, 1855; Krutzsch, 1966; Milewicz, 1985, 1997; Walaszczyk, 2008). Scupin (1910) suggested that the southeast-trending North Sudetic Basin was bordered by elevated island areas to the northeast and southwest, which he called the Ostsudetische Landmasse (East Sudetic Landmass) and Riesengebirgsinsel (West Sudetic Island), respectively. Scupin (1910), much like Partsch (1896) before, postulated a connection of the North Sudetic Basin with the Intra-Sudetic Basin to the southeast. Scupin (1913) recognized correctly the northwesterly transition of sandy deposits into mudstones and marlstones (cf. Figure 2) as the longitudinal direction of basin bathymetric deepening.

The notion of the Late Cretaceous basin's location between two Sudetic landmasses was supported by Andert (1934), although he postulated that the land area to the southwest—the Ostsudetische Landmasse of Scupin (1910)—comprised two islands, the Lausitz Insel and Riesengebirges Insel, which may have been periodically submerged. Apart from this hypothetical modification, the original palaeogeographic framework postulated for the North Sudetic Basin by Scupin (1910) remains valid.

The modern stratigraphic and palaeoenvironmental framework for the basin was developed by Milewicz (1956, 1965, 1966, 1973, 1985, 1997, 2006) and Milewicz *et al.* (1968), with subsequent contributions by Walaszczyk (2008), Leszczyński (2010, 2018) and Chrząstek and Wypych (2018). Particularly important was the recognition by Milewicz (1956) of a hiatus between the Rakowice Wielkie Formation and the Czerna Formation in the southeastern part of the basin (Figure 2), attributed to a northwesterly retreat of the sea from a large part of the basin and erosion in this emerged area. Walaszczyk (2008) later dated this event to the late mid-Coniacian and Leszczyński (2018) translated it as a forced regression in the parlance of sequence stratigraphy. Marine offshore sedimentation proceeded uninterrupted in the northwestern part of the basin until at least the middle Santonian (Milewicz, 1958, 1965, 1970, 1997, 2006; Walaszczyk, 2008).

Milewicz (1997) interpreted the Coniacian–Santonian succession in the North Sudetic Synclinorium as representing the latest regressive phase of a transgressive–regressive (T–R) cycle and the earliest transgressive phase of the next T–R cycle. Walaszczyk (2008) suggested that the Czerna Formation and coeval Węgliniec Formation (Figure 2) represent the final regressive phase of a complex series of minor T–R cycles. Leszczyński (2010) interpreted the Żerkowice Member of the Rakowice Wielkie Formation (Figure 2) as a regressive systems tract formed at the culmination of the regressive phase and separated by a hiatus from the overlying transgressive systems tract of a 3rd-order eustatic cycle. Leszczyński (2018) attributed deposition of the Żerkowice Member to the KCo1 eustatic event of sea-level fall (Haq, 2014).

5 | FIELD MATERIAL

The present study is based on the outcrop sections of 12 active or abandoned quarries and an isolated rock tor (Figure 1B, Table 1), as well as 31 pre-existing exploration borehole profiles, supplemented by core samples from eight boreholes (Figure 1B). The outcrops are located in the southeastern part of the North Sudetic Synclinorium, where the sandy Żerkowice Member is exposed and the sandstone quarries are located. Outcrops at Localities 5, 9 and 12 (Figure 1B) show the upper part (up to 90 m thickness) of the Żerkowice Member and the lower part (12–20 m thickness) of the Czerna Formation. Outcrops at the other localities show only the upper part (up to 15 m thickness) of the Żerkowice Member, with up to a few metres of the Czerna Formation exposed at Localities 1 and 4 (Figure 1B).

The data from boreholes are limited to lithology and sediment grain size (Figure 3), as the small-diameter and mainly poor-quality cores did not allow a reliable recognition of sedimentary structures. Detailed data on the bedding pattern, sedimentary structures, transport directions and trace fossils were collected from the outcrop sections (Figure 1B).

6 | METHODS AND TERMINOLOGY

Conventional field methods were used, such as a detailed logging, measurement of bedding attitude and palaeocurrent direction (mainly from cross-stratification), photographing of outcrop details and a line drawing of stratification architecture on outcrop photomosaics. Observations were made both in outcrop walls and in some loose rock blocks extracted by mining work. A review of the recorded sedimentary features is given in Figure 4 as a legend to outcrop logs.

The descriptive sedimentological terminology is according to Harms *et al.* (1975, 1982) and Collinson *et al.* (2006). Sedimentary facies (lithofacies) are distinguished by their macroscopic characteristics (Harms *et al.*, 1982; Walker, 1984). Spatially and genetically related lithofacies are regarded as lithofacies associations representing specific

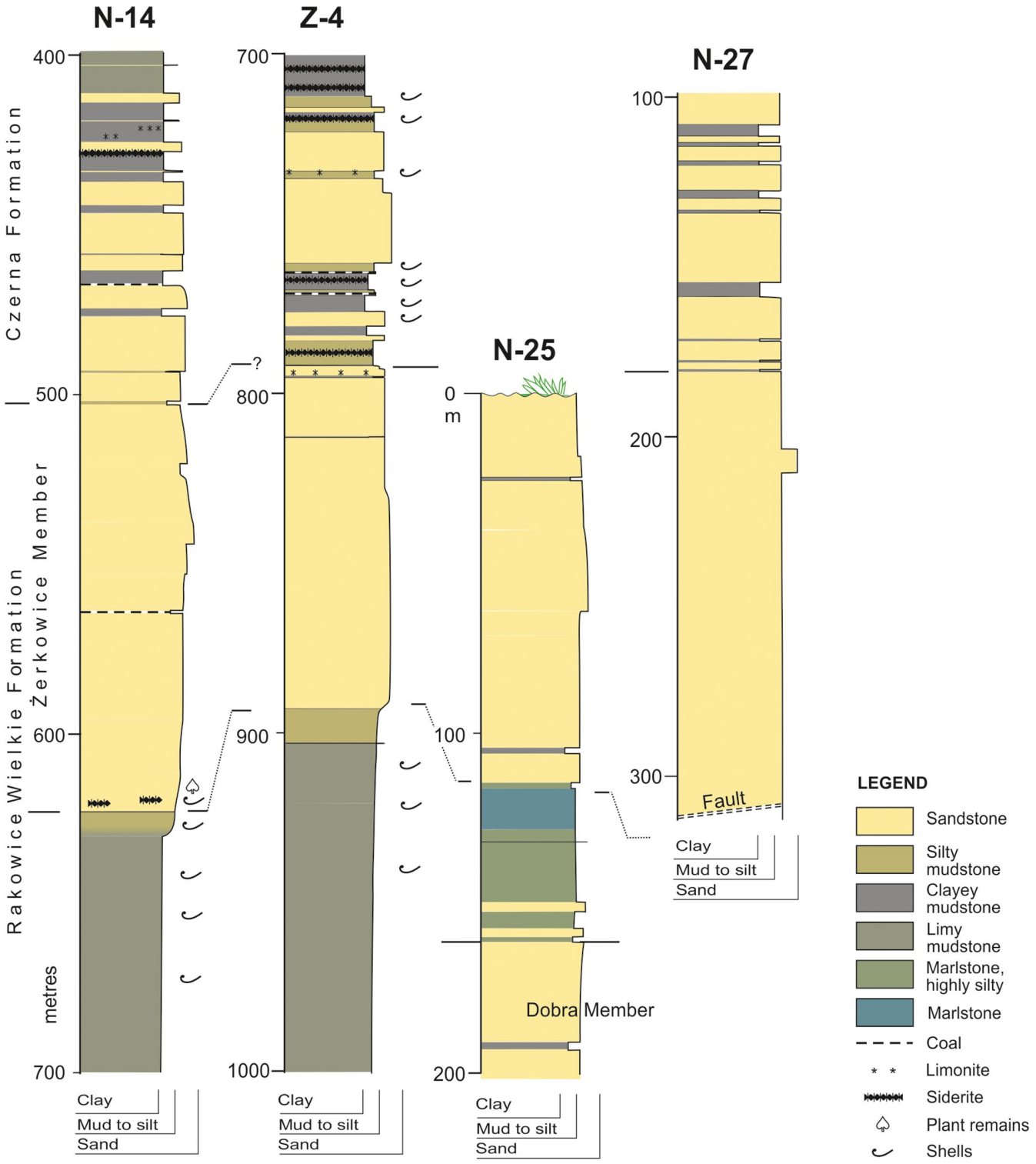

FIGURE 3 Borehole logs showing the stratigraphic transition of the Rakowice Wielkie Formation to the Czerna Formation; for borehole location, see Figure 1B. Log N-14 is based on Bossowski et al. (1976) and Bossowski (1991a); log Z-4 on Kochanowska (1988) and Leszczyński (2018); log N-25 on Dyja (1978) and Bossowski et al. (1978); and log N-27 on Bossowski et al. (1977)

sedimentary systems (environments). These assemblages are for simplicity given interpretive generic labels but their descriptions are separated from interpretations in the text.

The definitions of bioturbation structures and trace fossils (ichnofossils) are according to Bertling *et al.* (2006). The degree of sediment endichnial bioturbation is specified according to the bioturbation index (BI) scale of Taylor and Goldring (1993).

The basic concepts of sequence stratigraphy follow Catuneanu (2006) but Helland-Hansen's (2009) simplification

is used in distinguishing three basic types of systems tract as the building blocks of sequences: a forced-regressive systems tract (FRST) formed during relative sea-level fall; a transgressive systems tract (TST) formed during sea-level rise; and a normal-regressive systems tract, which may form during the sea-level highstand (HST) or lowstand (LST). The eustatic sea-level curve used for reference is from Haq (2014).

7 | THE ŻERKOWICE MEMBER

7.1 | Boundaries and thickness distribution

The Żerkowice Member is the uppermost lithostratigraphic division of the Rakowice Wielkie Formation in the southeastern part of the North Sudetic Synclinorium (Figure 2), where this sandy lithosome is exposed and has been subject to open-pit mining for a few centuries. The lower boundary of the Żerkowice Member is generally distinct, with the fine-grained quartzose sandstones overlying conformably, with a silty transition, a lithosome of dark-grey mudstones (Figure 3). The boundary is less distinct and rather controversial to the southeast, where (e.g., in borehole N-24, Figure 1B) the mudstone lithosome pinches out and the sandstones of the Żerkowice Member overlie directly the Dobra Member sandstones (cf. Figures 2 and 3; Bossowski, 1991b). The top of the sandy Żerkowice Member is the upper boundary of the Rakowice Wielkie Formation in the southeastern part of the synclinorium (Figure 2). This boundary is sharp and mainly erosional, with a stratigraphic hiatus (Figure 2) and with the sandstones overlain by a coal-bearing heterolithic unit dominated by mudstones and claystones (the Nowogrodziec Member of Milewicz, 1985), increasingly ferruginized towards the southeast and containing local patches of ferricrust or ferruginized fossil turf (e.g., at Locality 5, Figure 1B).

Exploration boreholes show the sandstone lithosome of the Żerkowice Member as thickening towards the northwest over a distance of 25 km along the synclinorium axis from 50 m between Localities 4 and 5, to 70 m between Localities 10 and 11 and up to 100 m in boreholes N-14 and N-26 (Figure 1B). Only a few kilometres farther to the northwest, in borehole N-27 (Figure 1B), the sandstone lithosome thickens abruptly to >200 m (corrected to >170 m on account of local tectonic tilt) and virtually pinches out in the nearby borehole J-1 (Figure 1B). This prominent thickening and abrupt pinch-out of the sandstone lithosome at its northwestern termination is meaningful, as discussed further in the paper.

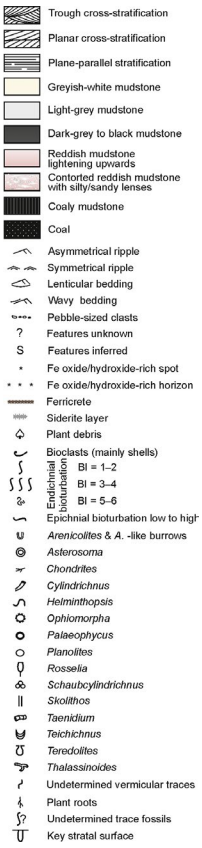

FIGURE 4 Review of sedimentological and ichnological features recognized in the Coniacian outcrops, given as a legend to the outcrop logs shown farther in this paper

7.2 | Lithofacies and trace fossils

The Żerkowice Member consists of fine to medium-grained and subordinately coarse-grained quartzose arenitic sandstones that are greyish white in colour, cream-yellow to light orange on weathered outcrop surfaces, and range from well cemented (mined as building blocks) to nearly soft (mined as glass sand). Mudstone interbeds are minor, thin and laterally discontinuous. Sand is mainly very well sorted, which commonly renders its internal stratification and bed boundaries poorly visible.

The volumetrically dominant lithofacies are sandstones with large-scale planar or trough cross-stratification (lithofacies Sc; Figure 5A through C). Cross-strata sets range from a decimetre to 3.2 m in thickness, show variable and often bidirectional transport directions and form laterally extensive cosets up to 15 m thick (Figures 6 and 7). Some cross-strata sets show hydroplastic deformation and partial homogenization by liquefaction. Subordinate lithofacies are sandstones with current ripple cross-lamination (lithofacies Sr, Figure 5A and J), wave-ripple cross-lamination (lithofacies Sw, Figure 5H and I) and plane-parallel stratification (lithofacies Sp, Figure 5D through F). Lithofacies Sr occurs as local intercalations, 5–50 cm thick, within the large-scale cross-strata cosets (Figure 5A). Lithofacies Sp and Sw commonly alternate with each other, forming units 0.1–4 m thick that split or cap the cross-strata cosets of lithofacies Sc (Figure 6, top). Lithofacies Sp dominates along the margins of the

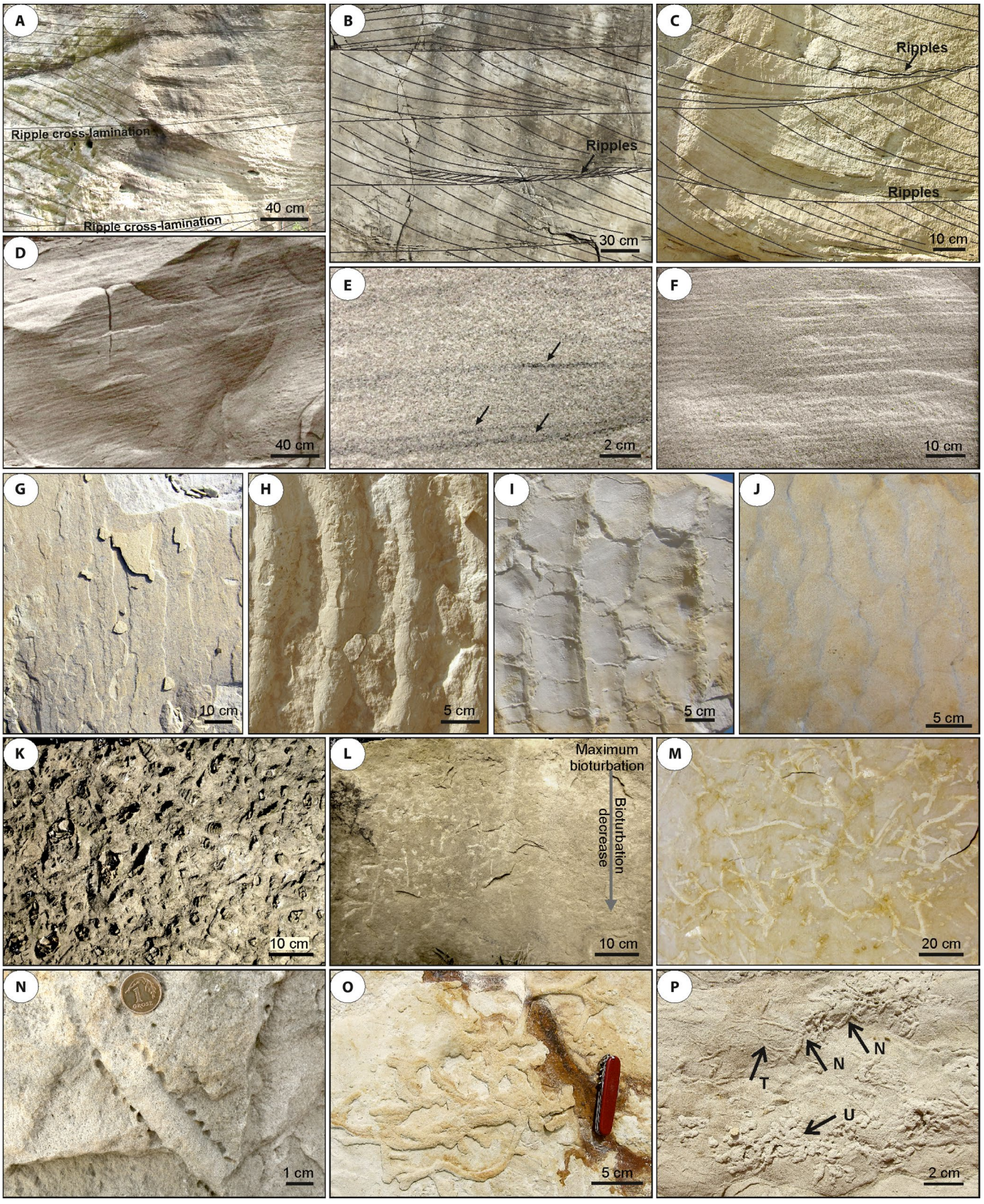

synclinorium, where it shows a gentle primary basinward inclination of 3–5° and forms basinward wedges up to 10 m thick. Where steeper inclined (10–15°, Figure 5D), the plane-parallel stratification shows primary current lineation (Figure 5G) and laminae rich in heavy minerals (Figure 5E). Clayey to silty grey mudstones (lithofacies M) are a minor component. This lithofacies occurs as thin (0.5–2 cm) and laterally discontinuous drapes between some of the cross-strata sets

FIGURE 5 Lithofacies and ichnofauna of the Żerkowice Member. (A) Sandstone with planar angular cross-stratification (lithofacies Sc) and interbeds of current ripple cross-lamination (lithofacies Sr) in vertical outcrop at Locality 7; transport direction to the right, obliquely towards the viewer. (B) Sandstone with planar tangential cross-stratification (lithofacies Sc) in vertical outcrop at Locality 6; note minor intrasets of reverse-flow ripple cross-lamination; main transport direction to the right, increasingly away from the viewer upwards. (C) Sandstone with trough cross-stratification (lithofacies Sc) in vertical outcrop at Locality 6; note minor intrasets of reverse-flow ripple cross-lamination; main transport direction to the right, obliquely away from the viewer. (D) Sandstone with gently inclined plane-parallel stratification (lithofacies Sp) in vertical outcrop at Locality 12. (E) Plane-parallel swash stratification in lithofacies Sp with dark laminae enriched in heavy minerals (arrows); vertical outcrop at Locality 12. (F) Sandstone with horizontal plane-parallel stratification (lithofacies Sp); vertical outcrop at Locality 12. (G) Parting lineation on bedding surface in a swash-stratified sandstone of lithofacies Sp at Locality 6. (H) Asymmetrical 2D wave ripples with rounded crests, exhumed on a bedding plane in sandstone lithofacies Sw at Locality 6. (I) Sharp-crested symmetrical 2D wave ripples exhumed on a bedding plane in sandstone lithofacies Sw at Locality 6. (J) 3D current ripples exhumed on a bedding plane in sandstone lithofacies Sr at Locality 6. (K) Shell lag (*Nerinea*) on a bedding plane in sandstone lithofacies Sp at Locality 4. (L) *Ophiomorpha* with a downwards decreasing density in sandstone lithofacies Sc at Locality 5. (M) *Ophiomorpha nodosa* network on sandstone bedding surface at Locality 5. (N) Subvertical *Ophiomorpha nodosa* in sandstone at Locality 4. (O) *Thalassinoides suevicus*, slightly flattened by compaction, on sandstone bedding plane at Locality 8. (P) ?*Nereites* isp., N; *Terptichnus* isp., T; and undetermined burrows, U, on sandstone bedding surface at Locality 6. Outcrop localities as in Figure 1B and Table 1

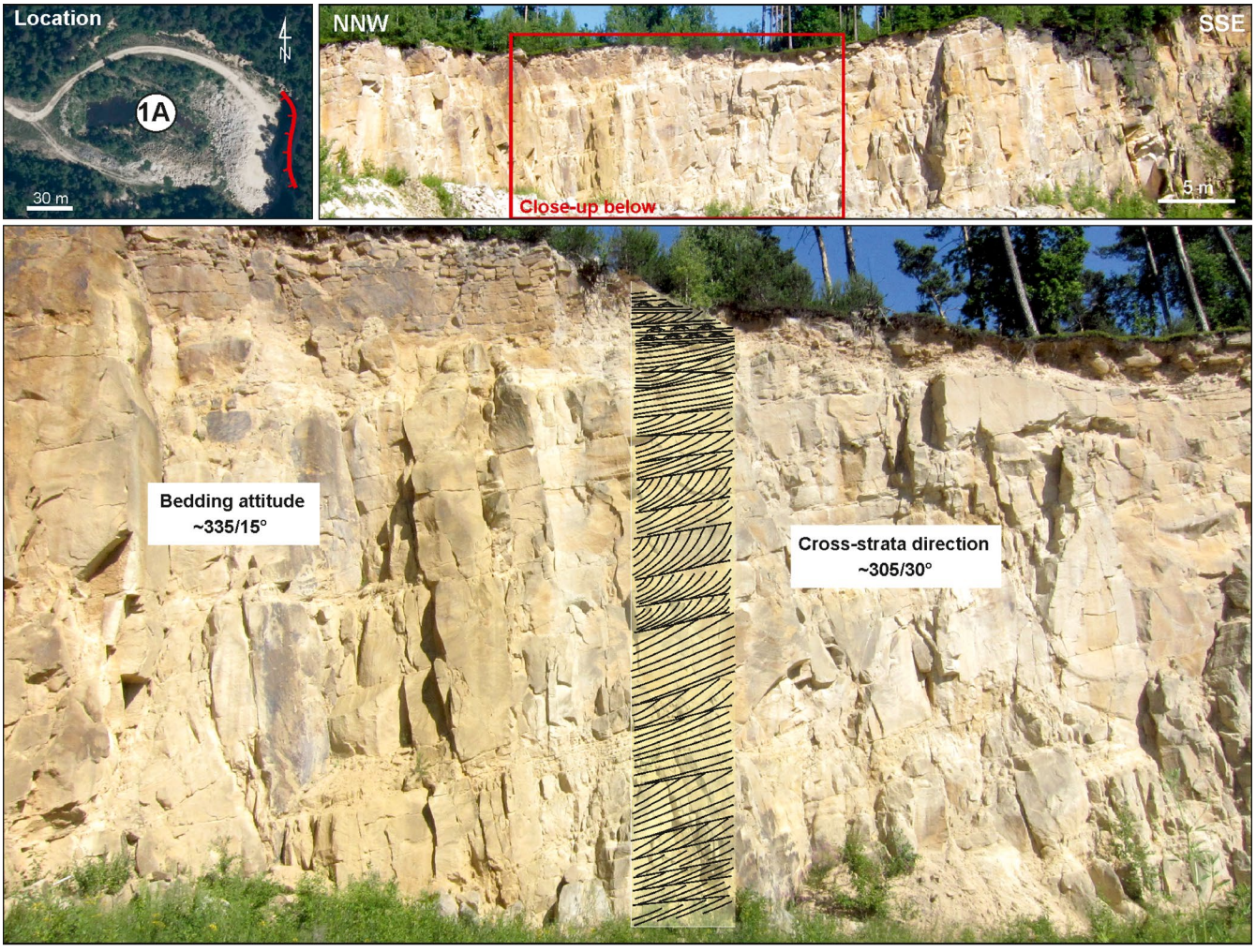

FIGURE 6 Succession of vertically stacked dune cross-strata sets (lithofacies Sc) interpreted as a northwest-trending longitudinal tidal bar (sand ridge). The bedding inclination at this locality includes at least 5° of secondary tectonic tilt. Locality 1 in Figure 1B, with the abandoned Czaple quarry 1A (Table 1) and cliff location shown in the inset image from Google Earth

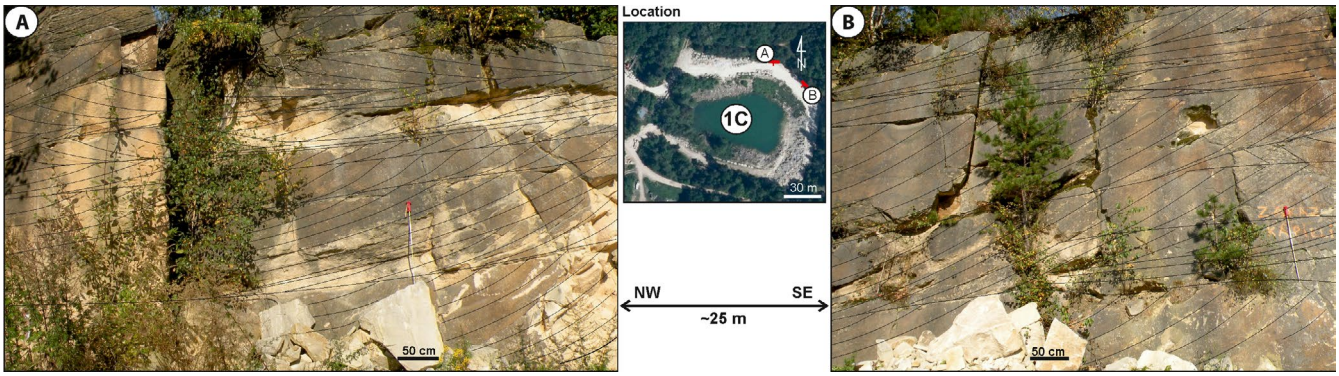

FIGURE 7 Succession of vertically stacked, bidirectional dune cross-strata sets (lithofacies Sc) interpreted as a northwest-trending longitudinal tidal bar (sand ridge). Outcrop photographs A and B show cliff portions of the abandoned Czaple quarry 1C (Table 1), as indicated in the inset image from Google Earth. Locality 1 in Figure 1B

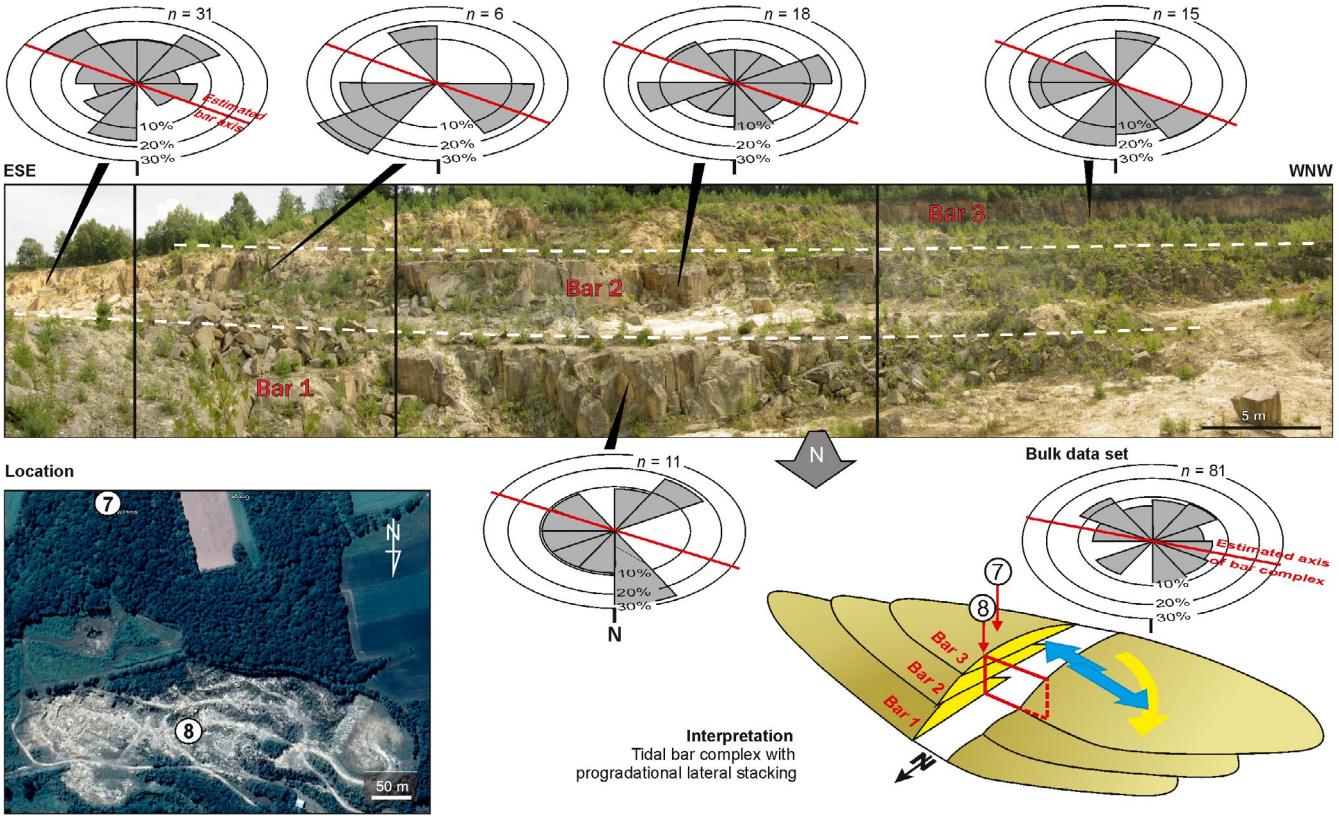

FIGURE 8 Succession of vertically stacked dune cross-strata sets (lithofacies Sc) interpreted as a complex of laterally superimposed, northwest-trending longitudinal tidal bars (sand ridges). The three bars (see interpretive diagram) are demarcated by dashed white lines in the outcrop photograph. The outcrop section was arbitrarily divided into four sectors (indicated by vertical black lines) in which the dip direction of cross-strata sets was measured for the individual bars, with the sector datasets summarized as rose diagrams (n = number of measurements). The inset image from Google Earth shows this abandoned Żerkowice quarry at Locality 8 (Figure 1B, Table 1) and the relative position of nearby Locality 7 where similar data were collected (see Figure 9)

of sandstone lithofacies Sc. Thicker mudstone units, up to 15 cm, are thinly interlayered with sand and/or silt, forming heterolithic beds (lithofacies H) beneath some of the sandstone cross-strata cosets.

Bioturbation occurs only locally (Milewicz, 1965, 1997; Bassyouni, 1984; Leszczyński, 2018). Burrows are concentrated as patches on the surfaces separating cross-strata cosets, especially where draped with mud, and in the topmost parts (10–15 cm) of cosets, that are often intensely bioturbated (BI 5–6) and show single burrows reaching down to nearly 1.5 m. Trace fossils include *Ophiomorpha* isp. (Figure 5L), *Ophiomorpha nodosa* (Figure 5M and N), *Thalassinoides*

suevicus (Figure 5O), *Nereites* isp., *Terptichnus* isp. and some small unidentified burrows (Figure 5P). The trace-fossil assemblages seem to range between a stressed expression of the *Skolithos* Ichnofacies and a proximal expression of the *Cruziana* Ichnofacies (Leszczyński, 2018). Body fossils are rare, represented by bivalves (mainly inoceramids), gastropods, ammonites and echinoids (Milewicz, 1965; Walaszczyk, 2008). Some crowded accumulations of marine snails *Nerinea* (Figure 5K) were found at Localities 4 and 5 (Leszczyński, 2010, 2018). Sporadically present at Localities 5, 6 and 8 (Figure 1B) are scattered wood fragments of various sizes, aggregated imprints of large fishbones(?), patchy shell pavements and discrete horizons rich in the imprints and casts of shell debris. Some large driftwood fragments are preserved solely as clustered *Teredolites*, the casts of wood-boring bivalves (Leszczyński, 2018).

7.3 | Lithofacies associations

7.3.1 | Basin-axis tidal bars

These sediment assemblages consist mainly of the cross-stratified sandstones of lithofacies Sc and form mounded sandbodies that are elongate roughly parallel to the synclinorium axis and virtually dominate the axial zone to the south-east (Figures 6 through 9). The quarry outcrops show these sandbodies as 5–15 m thick and apparently several kilometres long, stacked laterally and vertically into complexes up to 50 m thick (Figure 8). Their internal architecture shows vertically stacked two dimensional (2D) and three dimensional (3D) dune cross-strata sets, with the bedding surfaces (cross-set boundaries) slightly rising or subhorizontal and further gently falling to the northwest (Figures 6 and 7). Transport directions to the northwest locally dominate (Figure 6), with larger dunes overstepping smaller ones (Figure 7B) but the dune cross-sets are generally bidirectional (Figure 7A) and show a wide range of transport directions (see rose diagrams in Figures 8 and 9). Some cross-sets are underlain by local drapes of lithofacies M. Interbeds of lithofacies Sw and Sr are minor, with the latter showing mainly a reverse flow direction relative to that of the adjacent dune cross-strata (Figure 5A through C). The basal parts of sandbodies consist of smaller dune cross-sets (Figures 6 and 9) and are occasionally underlain by a heterolithic unit of lithofacies H, whereas their top parts are commonly packages of interbedded lithofacies Sp and Sw (Figures 6 and 9). Some of the sandbodies show shallow (up to 3 m) isolated palaeochannels at the top (Figure 10), filled with lithofacies Sc and trending slightly obliquely to the sandbody estimated long axis.

The elongate cross-stratified sandbodies are interpreted as longitudinal tidal bars, known also as tidal sand ridges

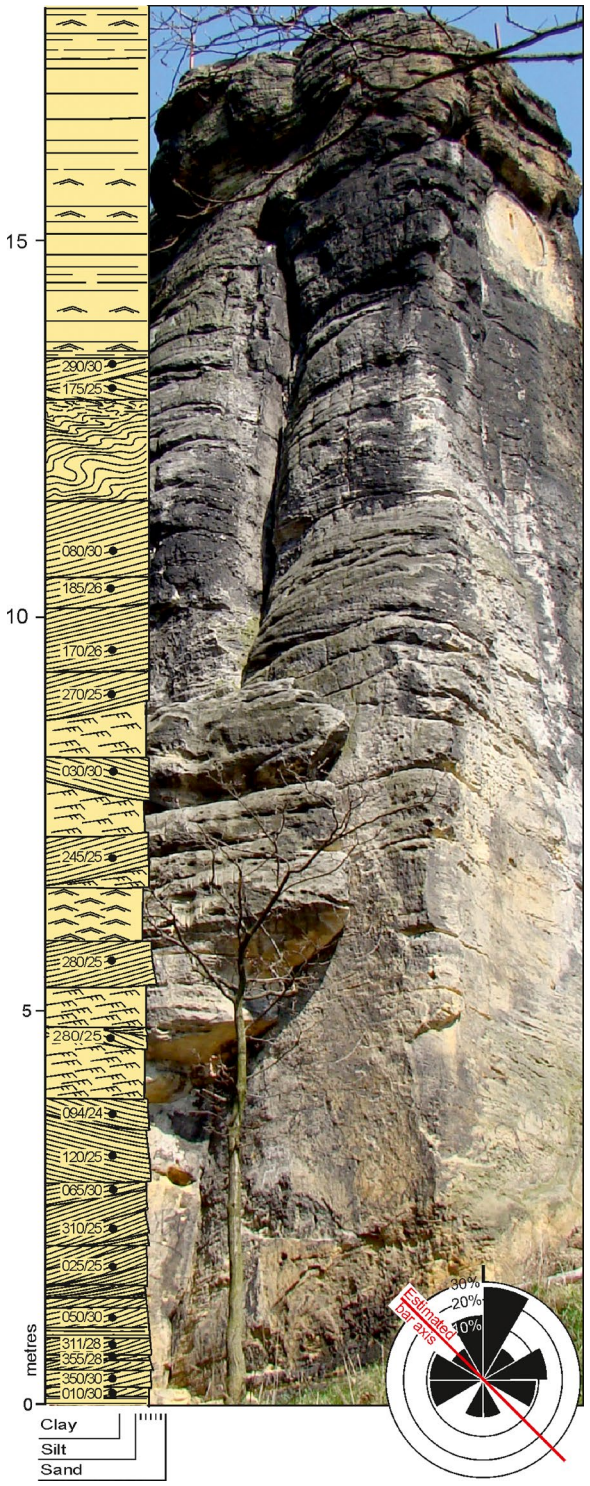

FIGURE 9 Succession of vertically stacked dune cross-strata sets of lithofacies Sc with interbeds of current-ripple and wave-ripple cross-laminated lithofacies Sr and Sw, increasingly wave-worked at the top (lithofacies Sw and Sp). The Medalion rock tor at Locality 7 (Figure 1B, Table 1; see also in the Google Earth image in Figure 8). The succession is thought to represent a shoaling-upwards bar no. 3 displayed in Figure 8 (see interpretive diagram therein). The inset rose diagram summarizes cross-strata palaeocurrent directions

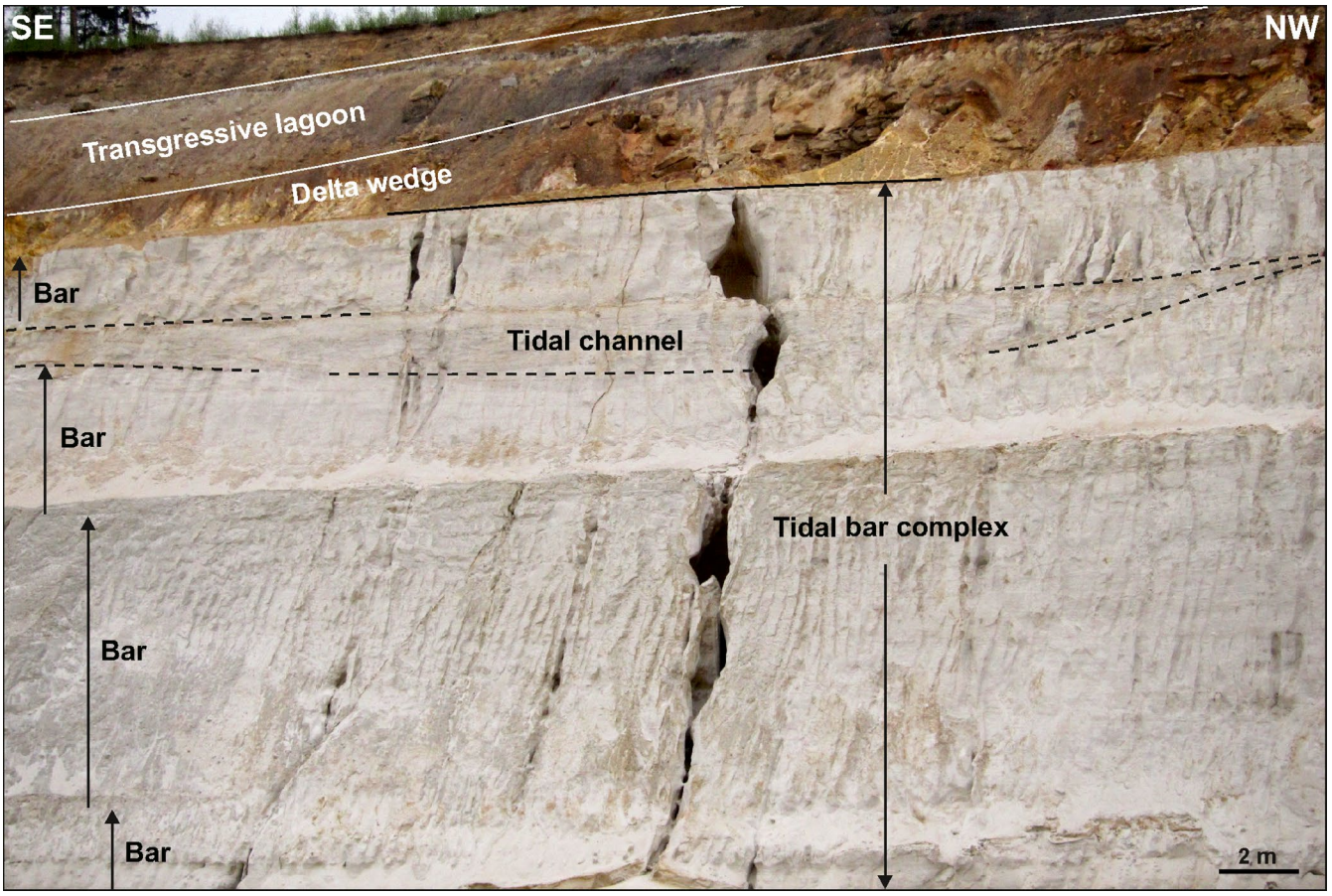

FIGURE 10 Portion of outcrop section in the Osiecznica quarry at Locality 12 (Figure 1B, Table 1). The topmost part of Żerkowice Member comprises a northwest-prograding tidal bar complex with an embedded tidal palaeochannel, overlain by a southwest-advancing basin-margin delta wedge. The overlying basal part of the Czerna Formation consists of transgressive lagoon deposits. For outcrop details, see Figure 15

(Figure 11A and B; Allen, 1982; Berné, 2000; McBride, 2003), which extend roughly parallel to the direction of tidal currents and grow seawards with a pronounced lateral migration component. They differ from transverse tidal bars, also called sandwaves or compound tidal dunes, which are approximately perpendicular to the currents (Houbolt, 1968; Dalrymple, 1984; Dalrymple and Rhodes, 1995; Berné, 2000; McBride, 2003; Olariu *et al.*, 2012). Tidal sand ridges are commonly associated with estuaries, tidal-inlet deltas, channel outlets in tide-dominated river deltas, narrow straits as well as open shelf environments (Houbolt, 1968; Swift, 1975; Reineck and Singh, 1980; Gaynor and Swift, 1988; Reynaud *et al.*, 1999a; Reynaud *et al.*, 1999b; Snedden and Dalrymple, 1999; Berné *et al.*, 2002; McBride, 2003; Longhitano and Nemec, 2005; Chiarella *et al.*, 2012; Longhitano *et al.*, 2014; Rossi *et al.*, 2017). Their component tidal dunes, as in the present case (lithofacies Sc in Figure 5A–C), range from 2D to 3D (cf. Longhitano *et al.*, 2014), commonly grow in thickness by overstepping one another (Figure 7B) and often show hydroplastic deformation of various origins (Chiarella *et al.*, 2016).

Unlike the sand ridges associated with estuarine river channels, the bars in the present case have non-erosional bases. They are often underlain by inter-bar muddy heterolithic lithofacies H (cf. Hein, 1987) and show an upward increase in flow energy (dune and grain sizes) indicating an aggradational shallowing culminating in the reworking by sea waves (Figures 6 and 9) after reaching the fairweather wave base. The alternation of lithofacies Sw and Sp in bar cappings indicates considerably fluctuating wave orbital velocity (Komar and Miller, 1975), possibly including episodic erosion by storm waves (Clifton and Dingler, 1984). The isolated palaeochannel features (Figure 10) are interpreted as tidal conduits cut over the sand-ridge top, probably to accommodate a storm-boosted local flow of tidal currents (cf. Dalrymple, 1984, 2010).

Based on the measurements from Localities 8 and 7 (Figures 8 and 9), the individual tidal bars show a mean thickness of dune cross-sets in the narrow range of 50–66 cm and a consistent median value of 40 cm (Table 2). The mean cross-set thicknesses are consistently higher than the median values (Table 2), which indicates a positively skewed thickness frequency distribution and implies a moderate excess of larger dunes. This is probably an effect of the local dune overstepping and thickness amplification (Figure 7B). The standard deviations (variability) of dune cross-set thickness show considerable bar-to-bar differences, in the range of 38–69 cm

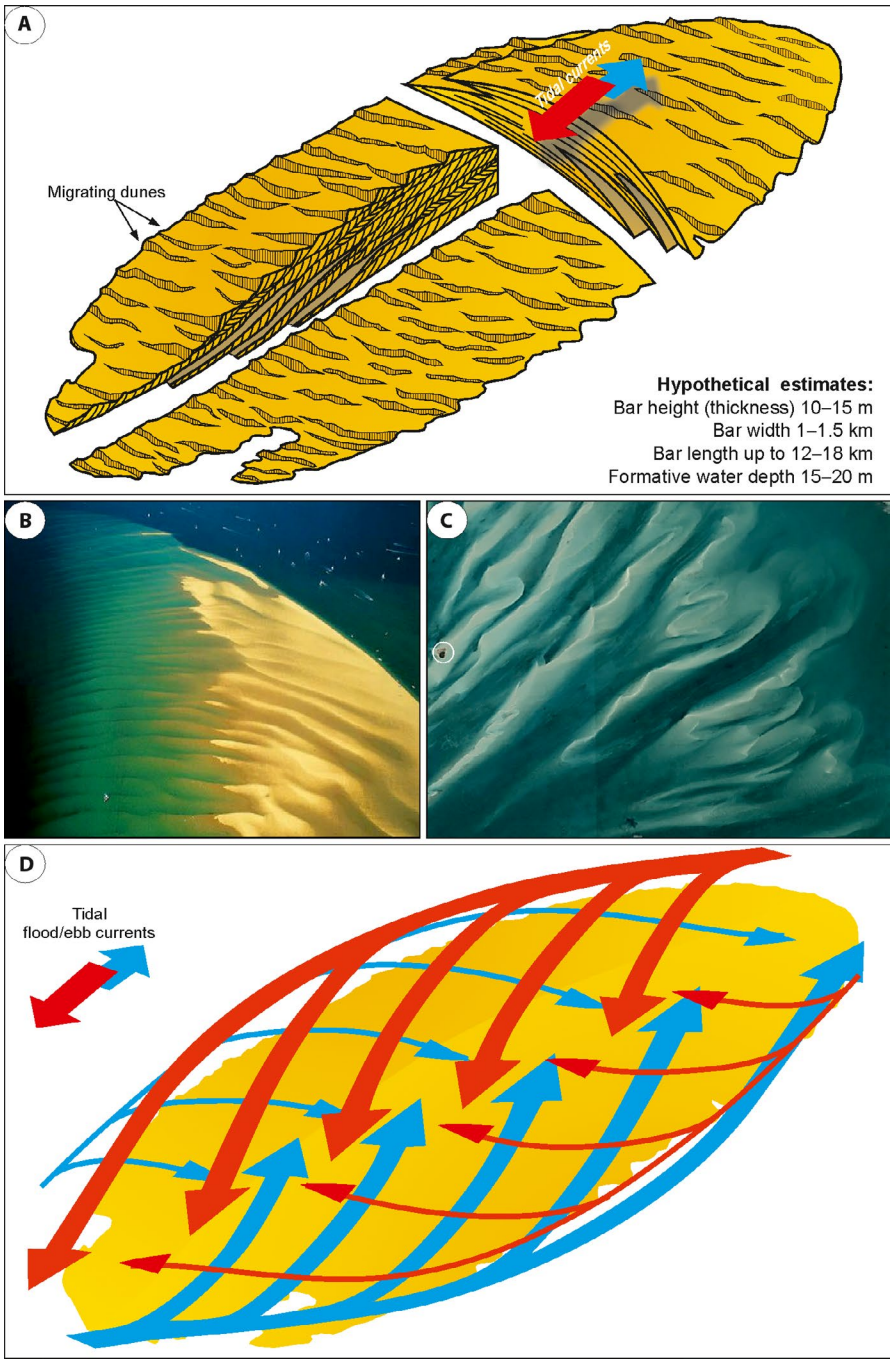

FIGURE 11 (A) Idealized model of a prograding longitudinal tidal bar (sand ridge) with the hypothetical estimates of bar dimensions and formative water depth pertaining to the Żerkowice Member. (B) Modern tidal sand ridge in the southern North Sea; the white spots on water surface (top right) are wakes of small motorboats. (C) An array of coalescing tidal sand ridges, fanning out from a strait in the Bahamas; large cruise ship (encircled) for scale. (D) Interpreted pattern of instantaneously reversing tidal currents over a tidal sand ridge inferred from palaeocurrent measurements (Figures 8 and 9). Photograph images from Google Earth

(Table 2), which is probably an artefact of the derivation of data from different parts of laterally stacked asymmetrical bars (cf. outcrop interpretation in Figure 8).

Modern case studies reviewed by McBride (2003) show that the height of tidal sand ridges may reach 40 m and their length and width are in the range of 5–120 km and 0.5–8 km, respectively. Based on the approximate equations given by McBride (2003), the bar maximum thicknesses measured in the present case (10–15 m) suggest bar lengths of 12–18 km and widths of 1–1.5 km, with the bar formative water depth of 15–20 m (Figure 11A). The acquired palaeocurrent data (rose diagrams in Figures 8 and 9) are broadly compatible with the flow pattern expected for tidal current instantaneous reversals over a sand ridge (Figure 11D; cf. Gaynor and Swift, 1988; Snedden and Dalrymple, 1999; Reynaud *et al.*, 1999a, b), while the lateral and vertical stacking of sand ridges into complexes (Figure 8) implies groups of coalescing adjacent coeval bars (Figure 11C).

7.3.2 | Basin-margin deltas

These are local wedge-shaped sediment assemblages composed of lithofacies Sp, with subordinate intercalations of lithofacies Sr and Sw and sporadic isolated dune cross-sets of

TABLE 2 Statistical summary of dune cross-set thicknesses in the tidal bar complex exposed at Locality 8 (Figure 8) and Locality 7 (Figure 9). Palaeobathymetric estimates are based on equations used by Dalrymple (2010)

Cross-set statistics	Dataset
	Bar 1
Number of data:	12
Median thickness:	40 cm
Mean thickness:	50 cm
Standard deviation:	48 cm
Estimated bathymetry:	4–29 m
	Bar 2
Number of data:	46
Median thickness:	40 cm
Mean thickness:	54 cm
Standard deviation:	38 cm
Estimated bathymetry:	5–31 m
	Bar 3
Number of data:	38
Median thickness:	40 cm
Mean thickness:	66 cm
Standard deviation:	69 cm
Estimated bathymetry:	6–38 m
	Total
Number of data:	96
Median thickness:	40 cm
Mean thickness:	58 cm
Standard deviation:	54 cm
Estimated bathymetry:	5–33 m

lithofacies Sc, which extend from the synclinorium outcrop margins towards its axis—transversely to the inferred tidal sand ridges and effectively interfingering with or onlapping the latter (Figures 12 to 15). The wedge-shaped sandbodies extend basinwards from both the southwestern (Figures 12 and 13) and the northeastern side (Figures 14 and 15) of the original synclinal basin, and their maximum thicknesses preserved near the synclinorium margins are up to 20 m. Common are drifted plant fragments. Trace fossils indicate mainly a shore-proximal expression of *Cruziana* Ichnofacies (Leszczyński, 2018).

These sandbodies are interpreted as basin-margin fluvial shoal-water deltas (sensu Leeder *et al.*, 1988; Postma, 1990) or mouth bar-type deltas (sensu Dunne and Hempton, 1984; Wood and Ethridge, 1988), dominated by river frictional effluent (lithofacies Sp; Wright, 1977) and fluctuating wave action (lithofacies Sp and Sw; Komar and Miller, 1975) with an influence of basin-axis tidal currents (lithofacies Sc; Dalrymple, 1984, 2010). The advancing deltas apparently impinged sidewise onto the basin-axis tidal bars (Figures 12 through 15). The shore-proximal subaerial parts of the deltas are scarcely preserved, removed by erosion of the synclinorium flanks (cf. Figure 14). The outcrop that comes closest to show a fluvial feeder system is that of the delta wedge at Locality 12 (Figure 15), where delta-top distributary palaeochannels are recognizable (see the top photograph, Figure 15), represented by coarser-grained cross-stratified sandstones (log interval 23–26 m in Figure 15) and interpreted as fluvial channel-mouth deposits.

7.3.3 | Basin-margin nearshore deposits

These sedimentary assemblages, much like the subaerial parts of basin-margin deltas, are only sparsely preserved and seldom exposed along the eroded margins of the synclinorium. They form another kind of basin-margin sand wedges, with preserved thicknesses of up to 5 m, which consist of the gently basinwards inclined (3–5°) deposits of alternating lithofacies Sp and Sw (log interval 6–10 m in Figure 16; intervals separating tidal bars in the log interval 0–20 m in Figure 15). Common are subtle angular unconformities in the form of planar erosional surfaces. The plane-parallel stratification in some units of lithofacies Sp is as steep as 10–15° (Figure 5D), showing heavy-mineral placers (Figure 5E) and primary current lineation (Figure 5G). Sand is nearly pure quartz, very well sorted and poorly cemented. Trace fossils are uncommon, representing an environmentally stressed version of the *Skolithos* Ichnofacies (Leszczyński, 2018).

These deposits are thought to represent a wave-dominated upper shoreface environment (Komar and Miller, 1975; Clifton and Dingler, 1984) of the basin shoreline that prograded from both sides of the basin jointly with the basin-margin local river deltas. Internal planar unconformities are attributed to episodic erosion by storm waves. The advancing shoreface deposits locally interfingered with the basin-axis tidal bars (Figure 15) and virtually buried them in some areas (Figure 16). The more steeply inclined packages of lithofacies Sp, with heavy-mineral placers and parting lineation, are interpreted as foreshore swash deposits (Allen, 1982), which would mean local encroachment of the basin shoreline (e.g. Figure 16, log interval 9.5–10 m).

8 | THE LOWER PART OF THE CZERNA FORMATION

8.1 | Basal boundary

The overlying Czerna Formation in the southeastern part of the North Sudetic Synclinorium is separated from the Żerkowice Member of the Rakowice Wielkie Formation by a

FIGURE 12 Outcrop section at Locality 1 (Figure 1B), in the active Czaple quarry 1B (see inset Google Earth image and Table 1), showing a basin-margin delta interfingering with the SW flank of basin-axis tidal sand bar (see inset interpretative diagram). The relic fluvial palaeochannel at the top represents forced regression that terminated deposition of the Żerkowice Member (cf. Figure 2)

FIGURE 13 Outcrop detail from Locality 1 (Figure 1B), the active Czaple quarry 1B (see inset Google Earth image and Table 1), showing a basin-margin shoal-water delta wedge onlapping the south-western flank of basin-axis longitudinal tidal bar

stratigraphic hiatus (Figure 2), which is an erosional unconformity that declines to the northwest along the basin axis and passes seawards into a correlative conformity (Milewicz, 1956, 1979; Walaszczyk, 2008). This erosional boundary demarcates a dramatic change in the sedimentary facies and depositional environment of the Coniacian North Sudetic Basin (Figures 3 and 15 to 17).

8.2 | Lithofacies and trace fossils

Mudstone lithofacies M is prominent directly above the basal boundary (Figures 3 and 15 to 17), forming units up to a few metres thick and ranging in colour from maroon and orange, with ferricrete concretions or bands up 5 cm thick, to greenish and dark grey with local siderite interlayers up to 7 cm thick. Some mudstone units are densely interspersed with sand and/or silt streaks and thin interlayers, forming a heterolithic lithofacies H that is often strongly bioturbated (BI 5–6) and occurs as units up to a few metres thick (Figures 16B and 18K to O). Mudstones are also intercalated with claystone lithofacies CL (Figures 15B and 18J) that forms units 0.1–1.2 m thick, ranging in colour from maroon and orange with ferricrete interlayers to greenish and dark grey or subordinately black (coaly).

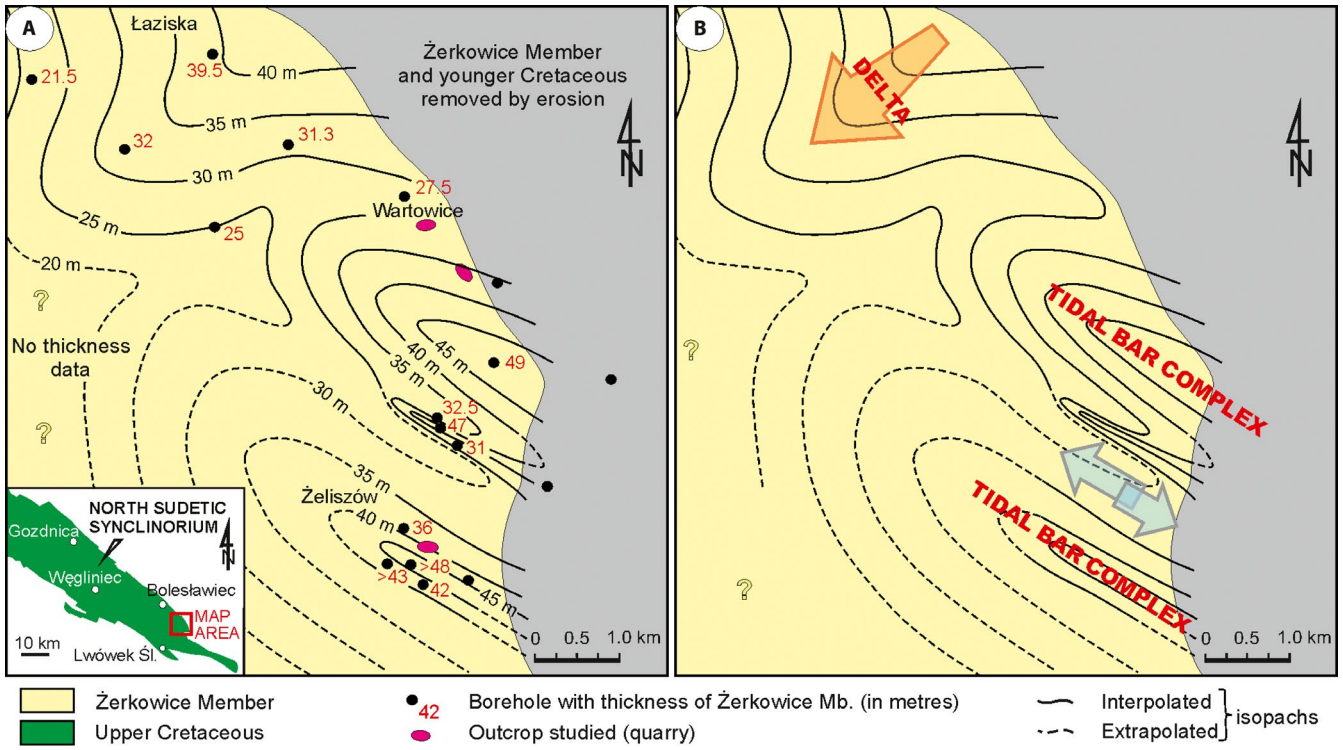

FIGURE 14 (A) Local sandstone isopach map of the Żerkowice Member (area indicated in the inset map), with the location of boreholes and the quarries in Wartowice (Locality 4) and Żeliszów (Locality 5); see localities in Figure 1B and Table 1; based on Drozdowski et al. (1978). (B) Interpretation of the isopach map as a basin-margin delta that interfered with the northwest-prograding tidal bar complexes. Note the large extent of basin-fill erosion due to the end-Cretaceous tectonic inversion

Another new facies are the coal beds of lithofacies C, up to 25 cm thick and ranging from autochthonous, underlain by seat-earth, to hypautochthonous (Figures 16C, 17 and 18D). Fine-grained, ripple cross-laminated sandstone beds of lithofacies Sr and Sw, 10–25 cm thick, occur as sheet-like intercalations in lithofacies H or are overlain by planar parallel-stratified sandstones of lithofacies Sp as upwards coarsening couplets 0.5–2 m thick (Figures 16A, 17 and 18E and F). Many sandstone beds are variably homogenized by bioturbation. Cross-stratified sandstones of lithofacies Sc are commonly medium to coarse-grained, with admixed granules and small pebbles. This lithofacies occurs solely as the infill of local palaeochannels, a few metres deep and less than 100 m wide, trending to the northwest and dominated by trough (3D dune) cross-stratification (Figures 17 and 18G).

Trace fossils abound, including rhizoliths, rhizocretions (Figure 18A) and densely plant root-penetrated palaeosols (Figure 18B and C) of vertisol to histosol type (cf. Retallack, 2001). Only some of the palaeosol horizons are actual seat-earths to coal beds (Figure 17). Common animal traces include *Ophiomorpha* (Figure 18I), *Palaeophycus* (Figure 18L), *Arenicolites* (Figure 18M), *Thalassinoides* and *Asterosoma* (Figure 18N). Leszczyński (2010, 2018) reported in detail on rich ichnofauna assemblages at Locality 9 (Figure 1B), while pointing to the sparse bioturbation at some other localities, such as the rare and taxonomically undetermined ichnofossils at Locality 12 (Figures 1B and 15). Leszczyński (2010) reported also on scattered mollusc shells, some buried in life position, and on shell lags preserved solely as imprints. Sporadic horizons with brackish-water bivalve and gastropod shells were described earlier by Drescher (1863) and Milewicz (1965, 1997).

FIGURE 15 Sedimentological log and corresponding outcrop photograph (top) of the upper part of Żerkowice Member and the lowermost Czerna Formation in the Osiecznica quarry at Locality 12 (Figure 1B, Table 1). Note the basin-margin delta wedge impinged sidewise onto the basin-axis tidal system at the top of the Żerkowice Member and the overlying transgressive lagoonal deposits of the basal Czerna Formation, split by a minor re-advance of the delta. For log legend, see Figure 4. Outcrop details (indicated at the log margin): (A) Sandy mouth bar of the coarsening-upwards minor deltaic wedge. (B) Muddy lagoonal deposits directly below this deltaic wedge. (C) Sandy mouth bar of the main delta wedge. (D) Bioturbated top of quasi-abandoned tidal bar. (E) Bidirectional dune cross-stratification in the tidal bar. (F) Gently northwest-descending tangential cross-strata sets in the lower part of the prograding tidal bar. (G) Plane-parallel stratification in the wave-worked upper part of the tidal bar

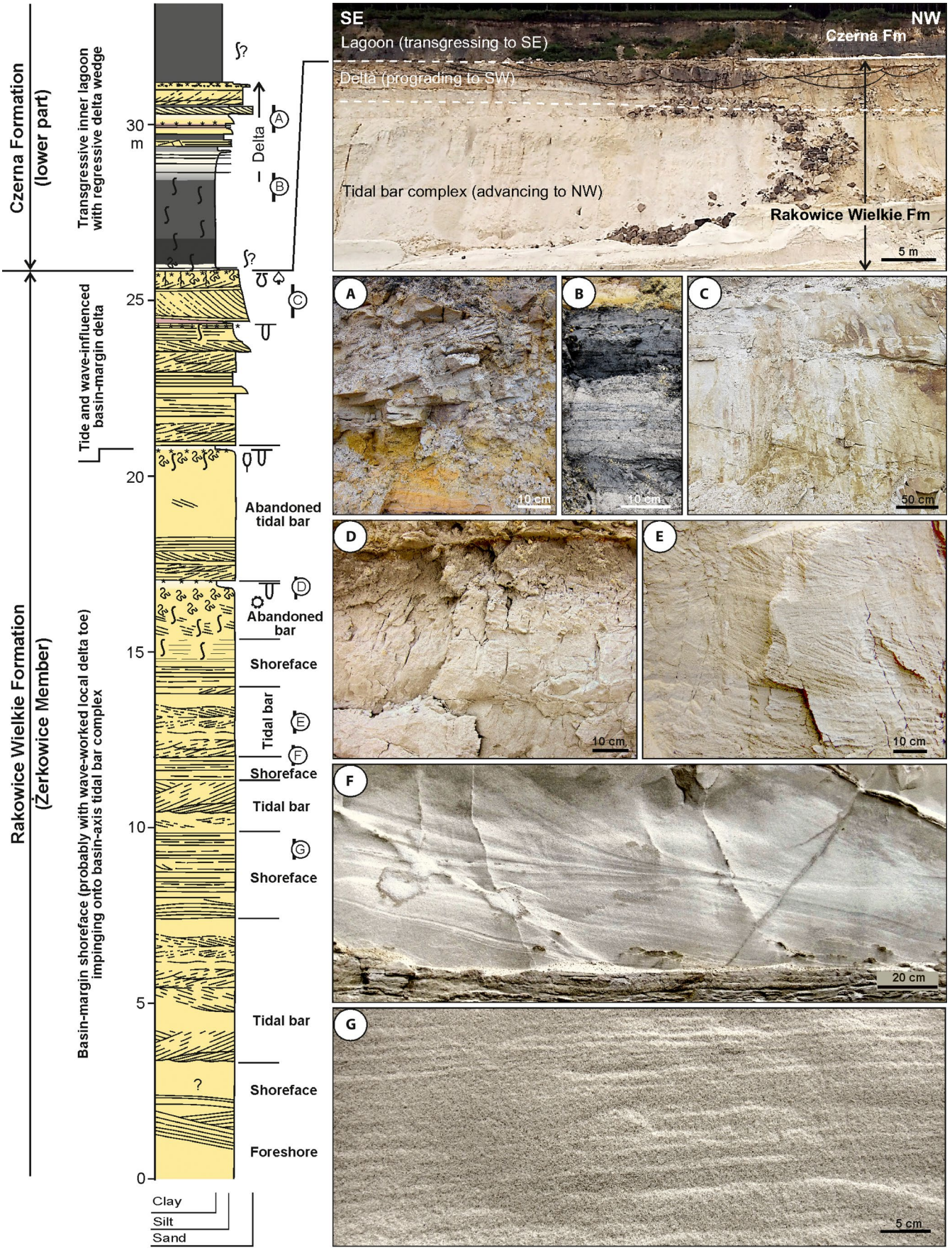
Czerna Formation (lower part)
Transgressive inner lagoon with regressive delta wedge
Rakowice Wielkie Formation (Żerkowice Member)
Tide and wave-influenced basin-margin delta
Basin-margin shoreface (probably with wave-worked local delta toe) impinging onto basin-axis tidal bar complex
30 m
25
20
15
10
5
0
Delta
Abandoned tidal bar
Abandoned bar
Shoreface
Tidal bar
Shoreface
Tidal bar
Shoreface
Tidal bar
Shoreface
Foreshore
Clay
Silt
Sand
SE
NW
Lagoon (transgressing to SE)
Delta (prograding to SW)
Tidal bar complex (advancing to NW)
Czerna Fm
Rakowice Wielkie Fm
5 m
A
B
C
D
E
F
G
10 cm
10 cm
50 cm
10 cm
10 cm
20 cm
5 cm

8.3 | Lithofacies associations

8.3.1 | Basal fluvial deposits

The lower boundary of the Czerna Formation, as a subaerial unconformity surface (Milewicz, 1956, 1979; Walaszczyk, 2008), is locally incised by northwest-trending isolated fluvial palaeochannels filled with lithofacies Sc (Figure 12), some influenced by tides before abandonment (Figure 17C).

These palaeochannels are interpreted as representing an incised fluvial drainage system directed along the basin axis towards the northwest and influenced frontally by marine tides. The incision of fluvial channels directly in littoral deposits (Figures 12 and 17C) strongly supports the notion of a forced regression.

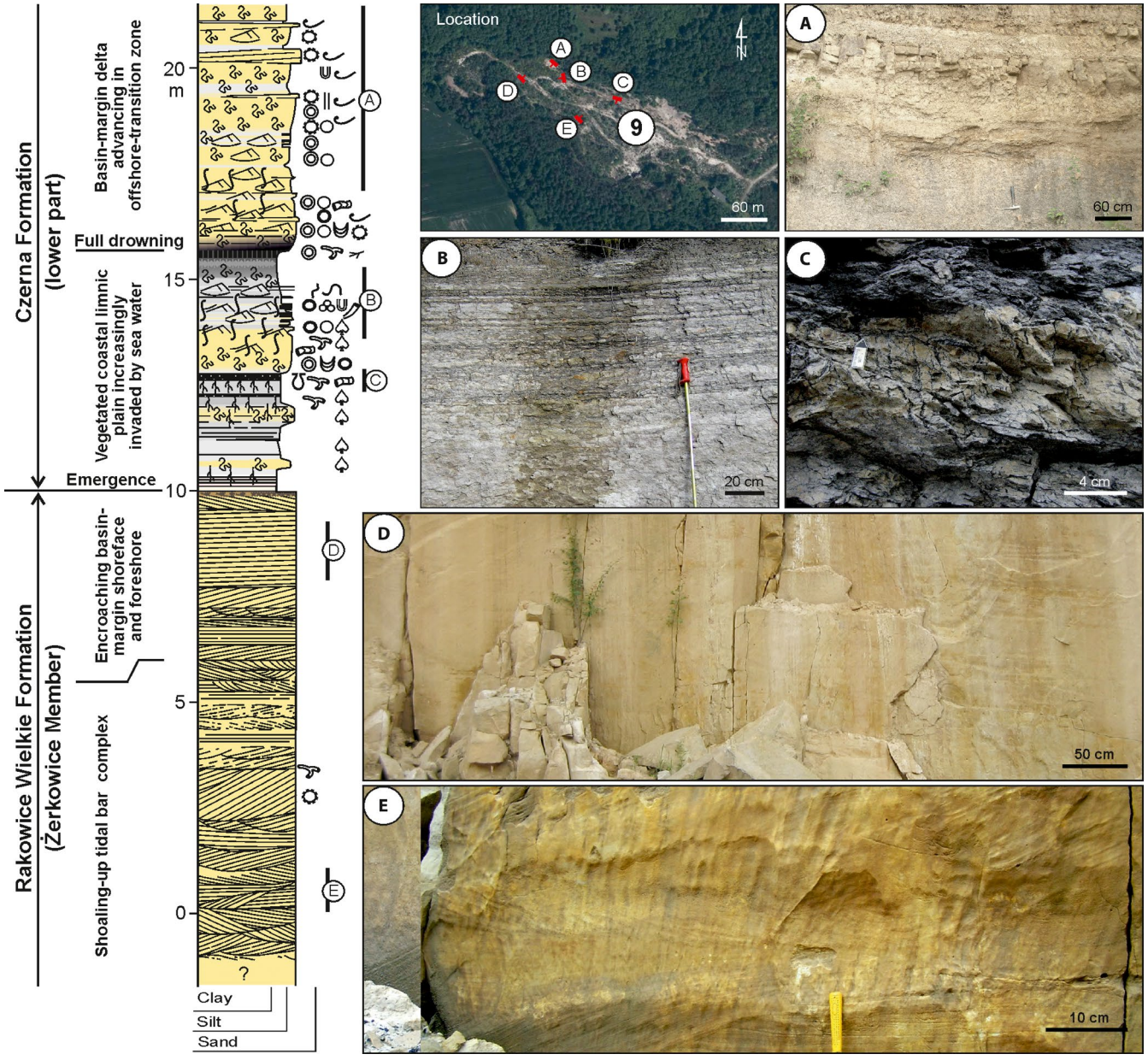

FIGURE 16 Sedimentological log of the uppermost part of the Żerkowice Member and lower part of the Czerna Formation in the Żerkowice quarry (Locality 9 in Figure 1B, Table 1). The tidal sand bar complex here was covered by a regressive sandy wedge of basin-margin shoreface to foreshore deposits prior to emergence. The overlying paralic deposits indicate gradual marine inundation and eventual full flooding, followed by encroachment of a basin-margin wedge of prodelta deposits. For log legend, see Figure 4. Outcrop details (indicated at the log margin and in the inset Google Earth image): (A) Coarsening-upwards packages of bioturbated progradational prodelta deposits of lithofacies Sr. (B) Thin-bedded, bioturbated lagoonal deposits of lithofacies H. (C) Muddy lagoonal deposits of lithofacies M with horizons of plant-root traces and brackish marine burrows. (D) Wave-worked upper shoreface sandstone of planar parallel-stratified lithofacies Sp. (E) Dune cross-stratified sandstone of lithofacies Sc

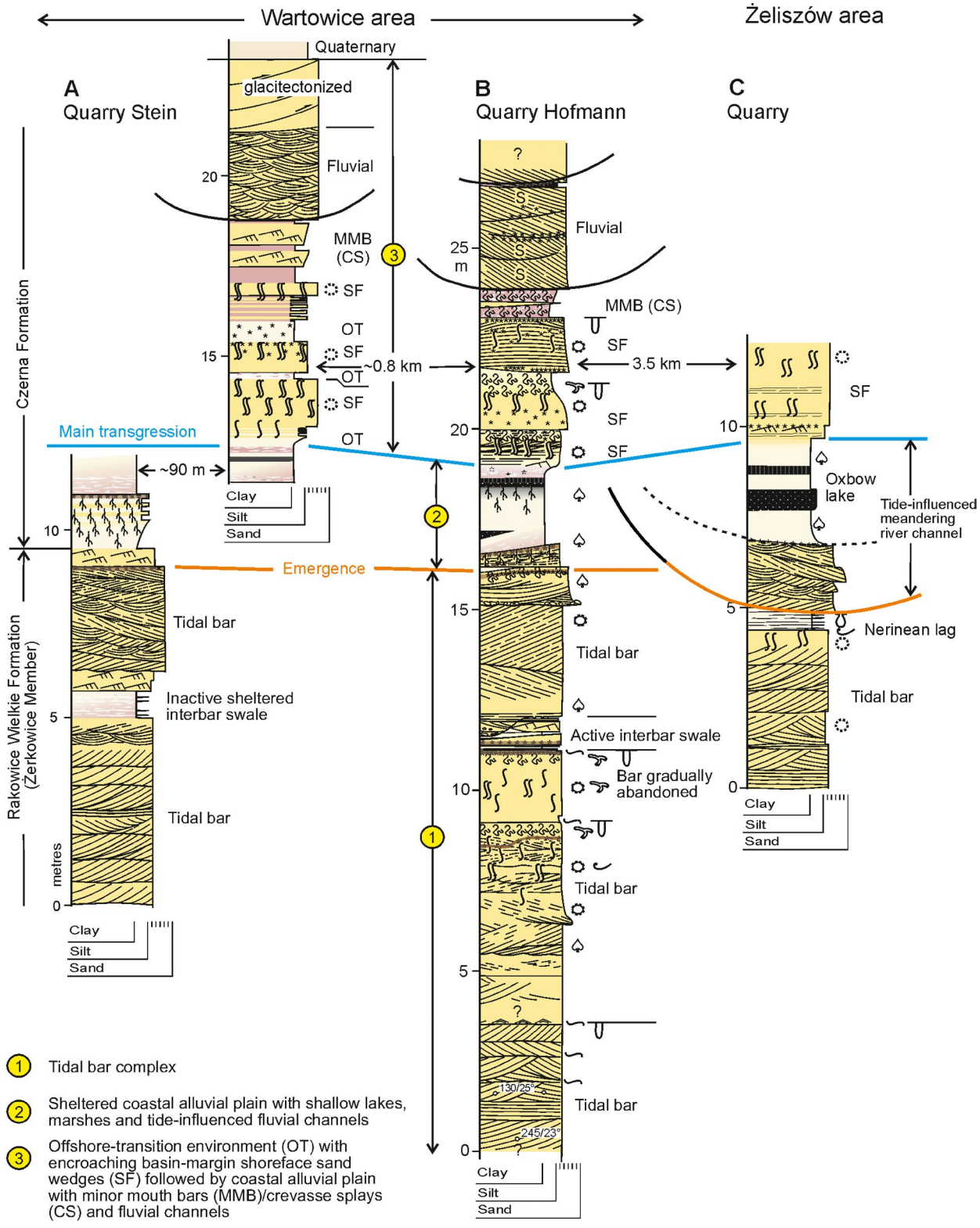

FIGURE 17 Sedimentological logs from quarries in Żeliszów and Wartowice (Localities 4 and 5 in Figure 1B and Table 1), showing the upward passage of the Żerkowice Member of the Rakowice Wielkie Formation to the Czerna Formation. Note that deposition of the Żerkowice Member was terminated by emergence, with the tide-influenced fluvial palaeochannel probably a time-equivalent of the fluvial palaeochannel at Locality 1 (Figure 12). The deposition of the Czerna Formation in this area commenced in a peat-forming terrestrial coastal-plain environment, which was eventually flooded by marine transgression. The subsequent highstand normal regression involved rapid advances of the basin-margin shoreface, culminating in the expansion of a basin-margin fluvio-deltaic system

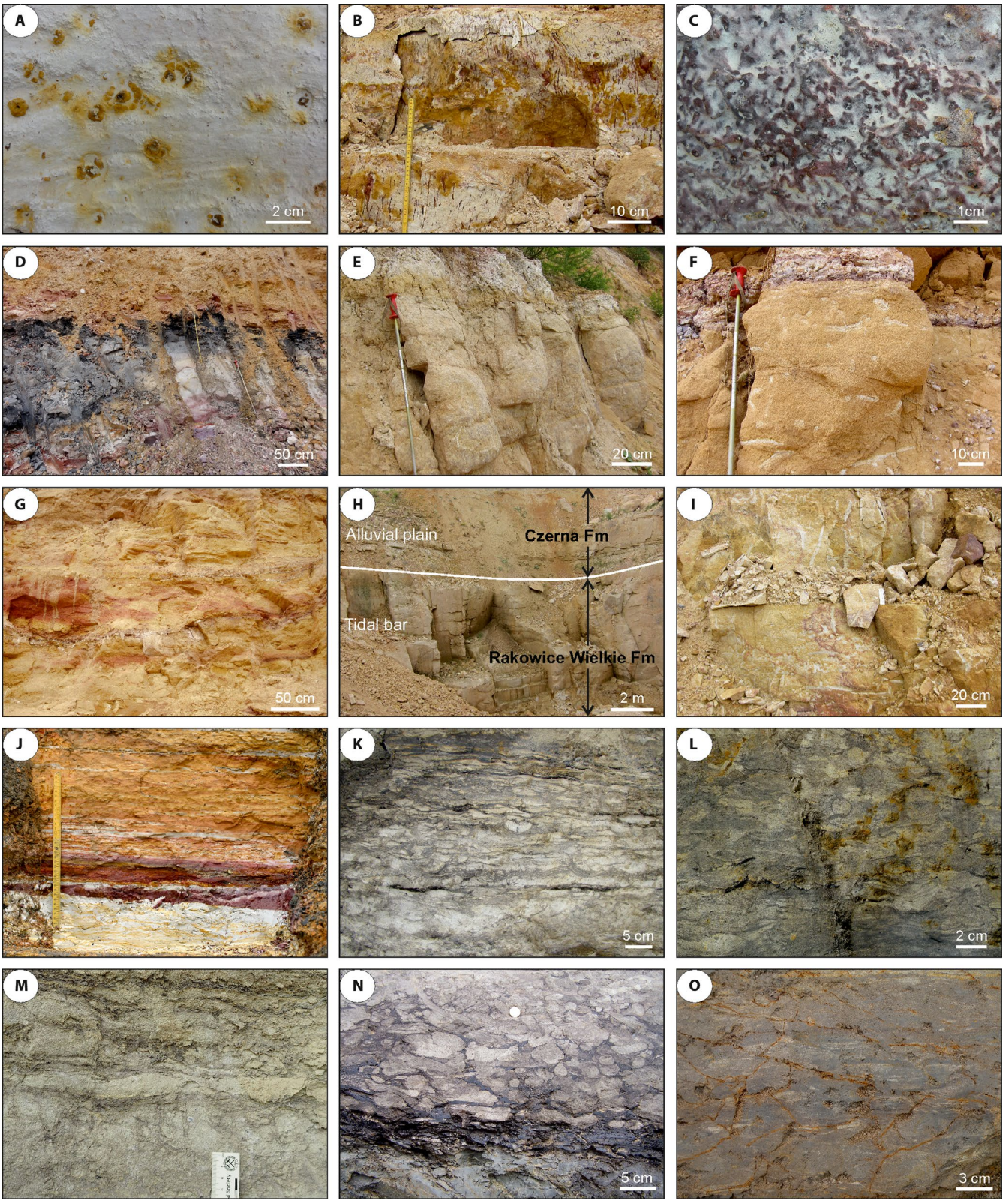

8.3.2 | Paralic limno-lagoonal deposits

The overlying sedimentary succession of the Czerna Formation commences with a widespread unit of fined-grained deposits, 2–5 m thick, dominated by lithofacies M, CL and H with subordinate intercalations of sandstone lithofacies Sr and with autochthonous or hypautochthonous coal beds of lithofacies C (Figures 15 through 17). Brackish shelly fauna and ichnofauna accompany palaeosols and accumulations of plant debris in this unit, locally even

FIGURE 18 Lithofacies and ichnofauna of the lower part of the Czerna Formation. (A) Rhizoconcretions and (B and C) denser plant-root penetration structures at the formation base at Locality 5 (Figure 17A). (D) Dark-grey claystone of lithofacies CL overlain by autochthonous coal of lithofacies C in the basal part of the formation at Locality 5 (Figure 17B). (E and F) The overlying shoreface lithofacies Sp at this latter locality (Figure 17B), showing a variable degree of bioturbation with *Ophiomorpha(*?). (G) Cross-stratified fluvial sandstone of lithofacies Sc in the top part of the outcrop at the same locality (Figure 17B). (H) Tidally influenced fluvial palaeochannel incised in the underlying formation at Locality 4 (Figure 17C). (I) *Ophiomorpha* in shoreface lithofacies Sp in the uppermost part of the outcrop at Locality 4 (Figure 17C). (J) Light-grey to reddish claystone with ferricrete (lithofacies CL) passing upwards into iron-stained yellowish mudstone (lithofacies M) in the formation basal part at Locality 9. (K) Lagoonal heterolithic deposits of lithofacies H at Locality 9, with (L) *Palaeophycus* and (M) *Arenicolites* burrows. (N) Prodelta heterolithic deposits of lithofacies H with *Thalassinoides* and *Asterosoma* burrows at Locality 9. (O) Offshore-transition lithofacies H at Locality 9, with interlayers of fine-sand lithofacies Sw heavily obliterated by bioturbation. Locality numbers as in Figure 1B and Table 1

directly at its base and within the same depositional bed. This unit of coal-bearing muddy deposits is presumably the Nowogrodziec Member of Milewicz (1985) (Figure 2).

Notable is the short-distance lateral variation in the thickness of this unit and in the relative proportion of its component lithofacies (cf. Figures 15 to 17). In the most distant quarry outcrop to the northwest (Locality 12, Figure 1B), this muddy unit is at least 9 m thick and split in the middle by a coarsening-upwards sandstone wedge, 2–4 m thick, composed of lithofacies Sr, Sp and Sc (Figure 15, top). The nearby boreholes N-14 and N-27 (Figures 1B and 3) show that this muddy unit pinches out abruptly along the basin axis towards the northwest by interfingering with a coeval prominent sandbody, a few tens of metres thick, resting directly on the sandstones of Żerkowice Member. This unexposed sandbody has drawn little attention from previous researchers and is somewhat enigmatic, as it pinches out only a couple of kilometres farther to the northwest in the adjacent borehole J-1 (Figure 1B; Marciński, 1970), where marine muddy offshore-transition to offshore deposits dominate.

This coal-bearing muddy unit with brackish/marine fauna is thought to represent a paralic environment comprising extensive shallow lakes with peat-forming mires and small stream deltas. The thick muddy deposits in the distal outcrop at Locality 12 (Figure 15 top) are considered to represent an expanding and aggrading transgressive lagoon intruded sidewise by a southwest-prograding basin-margin sandy delta wedge. The lagoon was apparently sheltered from the open sea by the thick and narrow 'enigmatic' sandbody recognized in boreholes N-14 and N-27 (Figure 3), interpreted herein as a cross-basinal transgressive coastal sand barrier (cf. Sanders and Kumar, 1975; Rampino and Sanders, 1981; Thom, 1984). It was probably the formation and in-place growth of this inferred coastal barrier that blocked the earlier fluvial drainage of the emerged southeastern part of the basin and turned this area into a peat-forming paralic lacustrine plain with local stream deltas.

8.3.3 | Offshore transition to fluvio-deltaic deposits

The exposed overlying deposits in the lower part of the Czerna Formation consist of muddy heterolithic lithofacies H intercalated with sheets of sandstone lithofacies Sr, Sp and minor Sw. They form coarsening-upwards or sporadically fining-upwards packages, 0.5–1.5 m thick (Figures 16 and 17) and variably bioturbated (BI 0–6). Palaeosols and coal beds are lacking. Abundant trace fossils indicate a spatially and temporarily varying mosaic of the *Teredolites, Skolithos* and *Cruziana* ichnofacies (Leszczyński, 2018). The uppermost exposed deposits are arrays of laterally and vertically stacked palaeochannels, 3–4 m deep and 100–120 m wide, filled with the cross-stratified sandstones of lithofacies Sc (Figure 17 top), mainly medium to coarse-grained.

This part of the sedimentary succession, little more than 10 m thick (Figures 16 and 17), is thought to represent a marine offshore-transition environment (cf. Howard and Reineck, 1981; Laprida *et al.*, 2007; Dashtgard *et al.*, 2009) that underwent rapid shallowing by a spasmodic encroachment of basin-margin shoreface and prodelta sand wedges (cf. Elliott, 1974; Laprida *et al.*, 2007). The shallowing of the marine environment, apparently driven by storms and deltaic river floods, culminated in the expansion of the basin-margin alluvial plain with small shoal-water deltas, fluvial channels and associated floodplain crevasse-splays (Figure 17, top).

9 | DISCUSSION

9.1 | Palaeogeographic development

The North Sudetic Basin formed as a narrow synclinal trough in the mid-Cretaceous, as an early side effect of the Alpine orogeny. The trough was open to the northwest to the East Brandenburg Basin of the Boreal marine province (Musstow, 1968; Ziegler, 1990; Voigt *et al.*, 2008). It was initially connected by a non-preserved strait to the southeast with the adjacent Intra-Sudetic Basin and Bohemian Basin of the Tethyan province (Figure 1A; Partsch, 1896; Scupin, 1910; Ziegler, 1990; Voigt *et al.*, 2008; Leszczyński, 2010, 2018; Mitchell *et al.*, 2010). The hypothetical strait is estimated to have been three to four-times narrower than the North Sudetic Basin itself (cf. Figure 19) and is thought to have acted as a sediment bypass zone funnelling confinement-enhanced tidal currents. Its existence is evidenced by the localized accumulation of

multiple, northwest-advancing tidal sand ridges in the southeastern head-part of the basin (cf. Longhitano, 2013).

The synclinal basin accumulated Late Cretaceous deposits before being tectonically inverted into the present-day North Sudetic Synclinorium (Figure 1B) by the regional climax of the Alpine orogeny at the end of the Cretaceous (Żelaźniewicz *et al.*, 2011). The present study focuses on the Coniacian stage of evolution of the North Sudetic Basin (Figure 2), when a combination of tectonic and eustatic forcing resulted in a dramatic change in the basin palaeogeography and sedimentary environment. The mid-Coniacian witnessed a 'world change' in the North Sudetic Basin, as discussed in the following reconstruction of the Coniacian development in the southeastern inner part of the basin (Figure 19).

The Coniacian North Sudetic Basin was a long and relatively narrow marine embayment open to the northwest, with a hypothetical bayhead inlet funnelling amplified tidal currents. The result was a northwest-directed advance of a basin-axis littoral sand platform built of amalgamated tidal sand ridges (Figure 19A; cf. Figure 11C). The lateral margins of the basin hosted a coeval wave-dominated sandy shoreline with local shoal-water stream deltas (Figure 19A).

It is pertinent to mention at this point that a vigorous tide-driven marine palaeocirculation in this Late Cretaceous Central European seaway linking the Boreal and Tethyan provinces was indicated by studies of the nearby Bohemian Basin (Voigt *et al.*, 2008; Mitchell *et al.*, 2010). The Imperial College Ocean Model (ICOM) in boundary-forced runs predicted a maximum sea floor shear stress of 0.8–6.6 N m^{-2} for the North Sudetic Basin (Mitchell *et al.*, 2010) and expected to be much higher for the basin's narrow bayhead inlet. The ICOM hydrodynamic simulations by Mitchell *et al.* (2010) predicted also a pattern of instantaneous bidirectional currents, which would correspond rather well with the palaeocurrent data from interpreted tidal sand ridges in the present study (Figures 8, 9 and 11D). The tidal exchange and intermixing of Boreal and Tethyan waters within the North Sudetic Basin was probably inhospitable to marine fauna, which may explain the relative sparsity of fauna in the sandstones of the Rakowice Wielkie Formation (Figure 2; cf. Gani et al., 2007).

The tide-dominated littoral sand platform, with sidewise impinging basin-margin shoreface and deltaic systems (Figure 19A), advanced along the basin axis to an estimated distance of about 70 km by the mid-Coniacian (Figure 19B)—when the Alpine tectonism abruptly closed the bayhead tidal inlet and uplifted the southeastern part of the basin. This regional tectonic event coincided with the KCo1 eustatic episode of major sea-level fall (Haq, 2014; see curve in Figure 2). The resulting forced regression made the emerged littoral platform subject to denudation and dissection by rivers, with the scant area of tide-influenced terrestrial sedimentation shrinking towards the contemporaneous shoreline (Figure 19C).

The subsequent onset of marine transgression driven by the KCo2 eustatic sea-level rise (Haq, 2014; see curve in Figure 2) turned the frontal edge of the basin's former littoral sand platform into an aggrading coastal sand barrier sheltering a limno-lagoonal paralic plain (Figure 19D) with a flourishing vegetation and common brackish fauna. This palaeoenvironment hosted deposition of the mud-rich and coal-bearing lithostratigraphic unit distinguished by Milewicz (1985) as the Nowogrodziec Member (Figure 2), although it is possible that some of the basal paralic deposits in this unit—like its basal isolated fluvial palaeochannels (cf. Figures 12 and 17C)—are local relics of the preceding forced regression (Figure 19C).

The aggrading transgressive barrier was eventually drowned by the sea (cf. Sanders and Kumar, 1975; Rampino and Sanders, 1981; Thom, 1984), whereby the sheltered limno-lagoonal plain to the southeast was abruptly flooded by the sea (cf. Figures 16 and 17) and turned briefly into a marine offshore-transition embayment (Figure 19E). As the rate of relative sea-level rise declined, the uplifted bayhead zone and basin margins yielded sediment causing rapid shoreline advance with a concentric encroachment of fluvio-deltaic systems (Figure 19F) and similar expansion of terrestrial alluvial plain (cf. top part of Figure 17A and B).

The transgressive coastal sand barrier (Figure 19D), unexposed and hypothetical, is invoked in the present reconstruction for two main reasons. Firstly, to explain the 'enigmatic' spatial thickness relationships of sandy and muddy lithosomes indicated by boreholes in this part of the basin (see text section 8.3.2). Secondly, to explain why the flat coastal plain, instead of being instantly drowned by the KCo2 eustatic transgression, was able to accumulate the 'sheltered' succession of coal-bearing limno-lagoonal deposits of the Nowogrodziec Member (sensu Milewicz, 1985).

FIGURE 19 Schematic interpretative reconstruction of Coniacian palaeogeography and sedimentation in the southeastern inner part of the North Sudetic Basin. (A) The littoral system of coalescing tidal sand ridges of the Żerkowice Member (Figure 2) progrades to the northwest, impinged on laterally by the basin-margin nearshore and deltaic sandy systems. (B) This tide-driven littoral sand platform reaches its maximum basinward extent, terminated by the closure of the basin bayhead tidal strait and a forced marine regression. (C) The emerged former littoral sand platform is denudated and incised by river channels, with the coastal area of paralic sedimentation shrinking basinwards; this stage of development marks the top of the Żerkowice Member. (D) The onset of subsequent eustatic sea-level rise creates a transgressive, aggrading coastal sand barrier at the outer edge of the former littoral sand platform, with a barrier-sheltered lagoonal to paralic bayhead alluvial plain. (E) The aggrading coastal sand barrier is eventually drowned by the sea, whereby the bayhead paralic plain becomes briefly an offshore-transition marine zone. (F) The rebounding sediment yield from the basin's elevated margins causes rapid shallowing by the lateral encroachment of nearshore and fluvio-deltaic systems; the diagram portrays the beginning of the late Coniacian normal-regressive advance of the Czerna Formation (cf. Figure 2)

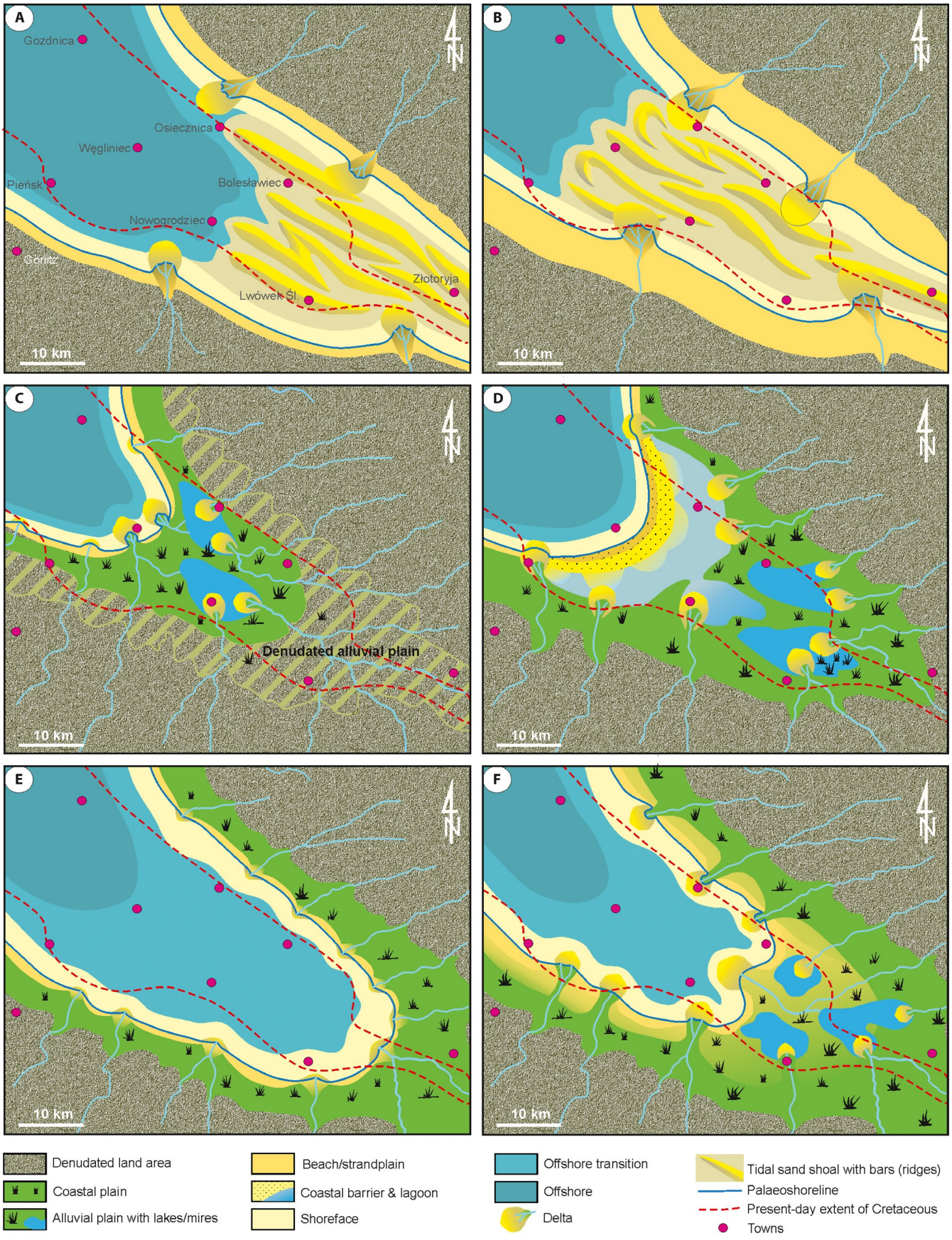
A
Gozdnica
Osiecznica
Węgliniec
Pieńsk
Bolesławiec
Nowogrodziec
Goritz
Złotoryja
Lwówek Śl.
10 km
B
10 km
C
Denudated alluvial plain
10 km
D
10 km
E
10 km
F
10 km
Denudated land area
Coastal plain
Alluvial plain with lakes/mires
Beach/strandplain
Coastal barrier & lagoon
Shoreface
Offshore transition
Offshore
Delta
Tidal sand shoal with bars (ridges)
Palaeoshoreline
Present-day extent of Cretaceous
Towns

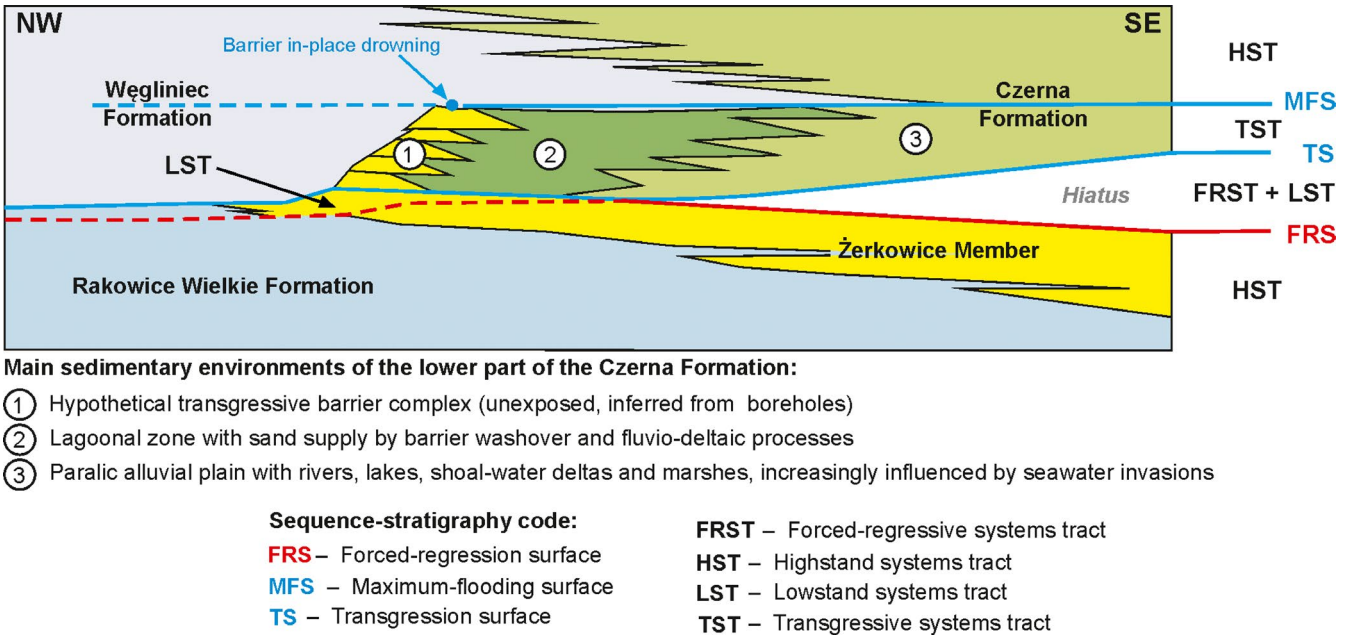

FIGURE 20 Sequence-stratigraphic interpretation of the Coniacian sedimentary succession in the southeastern part of the North Sudetic Basin, displayed as a basin longitudinal cross-section (schematic, not to scale). The hypothetical notion of an in-place aggrading and drowned transgressive coastal sand barrier (unexposed) is based on the great thickness of sandstones in borehole N-27 and their apparent lack in adjacent boreholes J-1 and W IG-1 only a few kilometres farther to the northwest along the basin axis (Figure 1B). For discussion, see text

9.2 | Sequence stratigraphy

The present study of the Coniacian succession in the North Sudetic Basin (Figure 19) encompasses stratigraphically the uppermost regressive sandstone wedge (Żerkowice Mb.) of the Rakowice Wielkie Formation and the lower transgressive to regressive part of the overlying Czerna Formation (Figure 2). This stratigraphic interval is crucial in the basin history, recording a dramatic change in the basin palaeogeography and sedimentary environment.

In terms of sequence stratigraphy (Figure 20), the Żerkowice Member represents a normal-regressive highstand systems tract (Figure 19A and B). Its development ended in a forced regression (Figure 19C) caused by a combination of regional tectonics and eustatic sea-level fall (cf. curve in Figure 2). The resulting erosional hiatus in the southeastern part of the basin passes into a correlative, normal-regressive deltaic lowstand systems tract in the unexposed northwestern part of the basin (Figure 20). The forced-regression unconformity is overlain by a transgressive systems tract represented by the Nowogrodziec Member of Milewicz (1985) and includes the hypothetical transgressive aggradational coastal sand barrier (Figures 19D and 20). Maximum marine flooding occurred with the barrier in-place drowning (Figures 19E and 20). The overlying exposed deposits of the lower Czerna Formation (Figure 17, upper part) represent a normal-regressive highstand systems tract (Figures 19F and 20).

In regional subsurface exploration, the thick and narrow 'enigmatic' sandbody found by boreholes N-14 and N-27 (Figures 1B and 3) was lumped stratigraphically with the sandy Żerkowice Member. In the present interpretation, this sandstone lithosome is an in-place drowned transgressive coastal sand barrier (Figure 20) belonging stratigraphically to the lowest part of the Czerna Formation as a lateral equivalent of the Nowogrodziec Member of Milewicz (1985) and being responsible for this member's accumulation.

It is worth noting that the Late Cretaceous pattern of marine transgressions and regressions in the North Sudetic Basin correlates rather well with eustatic sea-level changes (Figure 2), with the coincidental mid-Coniacian pulse of regional Alpine tectonism adding its critical effect to the eustatic impact on the basin. This Late Cretaceous record in the northern outer part of the Central European Boreal–Tethys seaway differs apparently from that in the midway-located Bohemian Basin to the south (Figure 1A; Voigt *et al.*, 2008; Uličný *et al.*, 2009; Mitchell *et al.*, 2010; Nádaskay and Uličný, 2014). The eustatic signal may have been obscured by the complicated topography and palaeogeography of this large basin and by a different local impact of the Alpine tectonism.

10 | CONCLUSIONS

The present study has reconstructed the Coniacian palaeogeography and palaeoenvironment of the North Sudetic Basin—a

synclinal trough within the Late Cretaceous Central European seaway linking the Boreal and Tethyan marine provinces. The basin formed in the mid-Cretaceous as an early regional side effect of the Alpine orogeny, and the Coniacian was a crucial stage in this basin's evolution and stratigraphic history.

The synclinal basin in the early Coniacian was a long and narrow shallow-marine embayment with a hypothetical bayhead strait funnelling amplified tidal currents. A littoral platform composed of coalescing tidal sand ridges prograded from the bayhead zone along the basin axis, while being impinged on from the sides by the basin-margin shoreface and deltaic systems.

A mid-Coniacian forced marine regression and closure of the bayhead strait, attributed to the regional Alpine tectonism combined with eustasy (KCo1 sea-level fall), brought about a dramatic change in the basin. The basin-wide littoral sand platform abruptly emerged and turned into a denudated terrestrial plain.

The late Coniacian eustatic marine transgression (KCo1/2 sea-level rise) formed an aggradational coastal sand barrier at the outer edge of the former littoral platform, sheltering a paralic limno-lagoonal environment with peat-forming mires. The inferred barrier was eventually drowned in-place by the sea, whereby the maximum marine flooding occurred, followed by a highstand normal regression recorded as a rapidly upwards-shallowing succession of offshore-transition to fluvio-deltaic deposits.

This case study of the sedimentation pattern in an evolving synclinal marine embayment, controlled by both eustasy and contractional tectonics, contributes to the existing facies models for estuarine embayments formed by a passive marine drowning of incised fluvial or glacial valleys and for tide-dominated marine extensional tectonic grabens. It is also a significant regional contribution to the understanding of the Late Cretaceous sedimentation in the Central European seaway linking the Boreal and Tethyan marine provinces.

ACKNOWLEDGEMENTS

The fieldwork of the first author (SL) was funded by a Jagiellonian University's DFG research grant, and of the second author (WN)—from a Bergen University's personal research account. For the permissions to do research in the sandstone quarries and to study their geological documentations, the authors thank the managements of the company Hofmann Natursteinwerke Polen GmbH, particularly B. Jarema and K. Gawron (quarries in Wartowice and Skała); the company Kamieniarz in Kielce (quarries in Nowa Wieś Grodziska, Czaple and Żeliszów); the company Kopalnie Piaskowca in Bolesławiec (quarries in Rakowice Małe and Żerkowice), particularly A. M. Sroka; and the company Kopalnia i Zakład Przeróbczy Piasków Szklarskich in Osiecznica, particularly K. Kasperczyk. The authors' gratitude for a free access to geological borehole documentations is extended to the directors and trustees of the National Geological Archives in Warszawa, the Geological Archives of the Geological Enterprise Proxima in Wrocław and the Geological Archives of the Lower Silesian Voievodeship in Wrocław. The manuscript benefited from the critical reviews by Domenico Chiarella, Sergio Longhitano and Guy Plint and from the editorial comments by Sam Purkis and Peter Swart.

CONFLICT OF INTEREST

No conflict of interest to declare.

DATA AVAILABILITY STATEMENT

All data from outcrops have been acquired by the authors and are displayed in the article figures. Borehole data are from public archives, as stated in the Acknowledgements.

ORCID

Wojciech Nemec https://orcid.org/0000-0002-9201-6071

REFERENCES

Allen, J.R.L. (1982). *Sedimentary Structures: Their Character and Physical Basis, Vol. 2. Developments in Sedimentology, 30B*. Amsterdam, Netherlands: Elsevier, pp. 643.

Andert, H. (1934) Die Fazies in der sudetischen Kreide unter besonderer Berücksichtigung des Elbsandsteingebirges. *Zeitschrift der Deutschen Geologischen Gesellschaft*, *86*, 617–637.

el Bassyouni, A.A.F.E. (1984) Sedimentology of the Upper Cretaceous sandstones of the North Sudetic Basin in the area between Złotoryja, Wleń and Lwówek Śląski. Wrocław, Poland: Archives of the Wrocław University.

Berné, S. (2000) Architecture, dynamics and preservation of marine sandwaves (large dunes). In Trentesaux, A. and Garlan, T. (Eds.) *Marine Sandwave Dynamics. International Workshop*. France: University of Lille 1, pp. 43–46.

Berné, S., Vagner, P., Guichard, F., Lericolais, G., Liu, Z., Trentesaux, A. *et al.* (2002) Pleistocene forced regressions and tidal sand ridges in the East China Sea. *Marine Geology*, *188*, 293–315.

Bertling, M., Braddy, S.J., Bromley, R.G., Demathieu, G.R., Genise, J., Mikulaš, R. *et al*. (2006) Names for trace fossils: a uniform approach. *Lethaia*, *39*, 265–286.

Beyrich, E. (1849) Das Quadersandsteingebirge in Schlesien. *Zeitschrift der Deutschen Geologischen Gesellschaft*, *1*, 390–393.

Beyrich, E. (1855) Ueber die Lagerung der Kreideformation im schlesischen Gebirge. *Abhandlungen der Königlichen Akademie der Wissenschaften zu Berlin*, *26*, 57–80.

Bossowski, A. (Ed.) (1991a) Wykroty N-14. *Profile Głębokich Otworów Wiertniczych Państwowego Instytutu Geologicznego, 72*, pp. 1–45. [In Polish.].

Bossowski, A. (Ed.) (1991b) Bolesławiec N-24. *Profile Głębokich Otworów Wiertniczych Państwowego Instytutu Geologicznego, 73*, pp. 1–64. [In Polish.].

Bossowski, A., Kossowska, I., Kuralowa, K. and Żołnierz, J. (1976) Poszukiwanie rud miedzi w rejonie niecki północnosudeckiej. Dokumentacja wynikowa otworów N-14 Wykroty, N-26 Osiecznica i N-19 Bielawa Górna. National Geological Archives, No. 122341. PIG, Warszawa. [In Polish.].

Bossowski, A., Kossowska, I. and Żołnierz, J. (1977) Poszukiwanie rud miedzi w rejonie niecki północnosudeckiej. Dokumentacja wynikowa otworu N-27 Parowa i stref rudnych z otworów Poświętne IG-2 i Borowe IG2. National Geological Archives, No. 122860. PIG, Warszawa. [In Polish.].

Bossowski, A., Bałazińska, J., Kossowska, I., Kural, K. and Cieśla, E. (1978) Poszukiwanie rud miedzi w rejonie niecki północnosudeckiej. Dokumentacja wynikowa otworów N-24 Bolesławiec i N-25 Osieczów. National Geological Archives, No. 2960. PIG, Warszawa. [In Polish.].

Boyd, R., Dalrymple, R. and Zaitlin, B.A. (1992) Classification of clastic coastal depositional environments. *Sedimentary Geology*, *80*, 139–150.

Catuneanu, O. (2006) *Principles of Sequence Stratigraphy*. Amsterdam, Netherlands: Elsevier, p. 375.

Chiarella, D., Longhitano, S.G. and Muto, F. (2012) Sedimentary features of the Lower Pleistocene mixed siliciclastic-bioclastic tidal deposits of the Catanzaro Strait (Calabrian Arc, south Italy). *Rendiconti Online della Società Geologica Italiana*, *21*, 919–920.

Chiarella, D., Moretti, M., Longhitano, S.G. and Muto, F. (2016) Deformed cross-stratified deposits in the Early Pleistocene tidally-dominated Catanzaro strait-fill succession, Calabrian Arc (Southern Italy): triggering mechanisms and environmental significance. *Sedimentary Geology*, *344*, 277–289.

Chrząstek, A. and Wypych, M. (2018) Coniacian sandstones from the North Sudetic Synclinorium revisisted: palaeoenvironmental and palaeogeographical reconstructions based on trace fossil analysis and associated body fossils. *Geologos*, *24*, 29–53.

Clifton, H.E. and Dingler, J.R. (1984) Wave-formed structures and paleoenvironmental reconstruction. *Marine Geology*, *60*, 165–198.

Cohen, K.M., Finney, S.C., Gibbard, P.L. and Fan, J.-X. (2013) The ICS international chronostratigraphic chart. *Episodes*, *36*, 199–204.

Collinson, J.D., Mountney, N.P. and Thompson, D.B. (2006) *Sedimentary Structures*, 3rd edition. Harpenden, UK: Terra Publishing.

Dalrymple, R.W. (1984) Morphology and internal structure of sandwaves in the Bay of Fundy. *Sedimentology*, *31*, 365–382.

Dalrymple, R.W. (2010). Tidal depositional systems. In James, N.P. and Dalrymple, R.W. (Eds.) *Facies Models 4*. St. John's, Canada: Geological Association of Canada, pp. 201–232.

Dalrymple, R.W. and Rhodes, R.N. (1995). Estuarine dunes and bars. In Perillo, G.M.E. (Ed.) *Geomorphology and Sedimentology of Estuaries. Developments in Sedimentology, 53*. Amsterdam, Netherlands: Elsevier, pp. 359–422.

Dalrymple, R.W., Zaitlin, B.A. and Boyd, R. (1992) Estuarine facies models; conceptual basis and stratigraphic implications. *Journal of Sedimentary Research*, *62*, 1130–1146.

Dalrymple, R.W., Zaitlin, B.A. and Boyd, R. (Eds.) (1994) Incised-Valley Systems: Origin and Sedimentary Sequences. *Society for Sedimentary Geology (SEPM) Special Publication, 51*,pp. 391.

Dalrymple, R.W., Leckie, D.A. and Tillman, R.W. (Eds.) (2006) Incised Valleys in Time and Space. *Society for Sedimentary Geology (SEPM) Special Publication, 85*,pp. 343.

Dashtgard, S.E., Gingras, M.K. and MacEachern, J.A. (2009) Tidally modulated shorefaces. *Journal of Sedimentary Research*, *79*, 793–807.

Drescher, R. (1863) Ueber die Kreide-Bildungen der Gegend von Löwenberg. *Zeitschrift der Deutschen Geologischen Gesselschaft*, *14*, 291–366.

Drozdowski, S., Engel, W. and Falecki, W. (1978) Dokumentacja geologiczna złoża rud miedzi Wartowice w kategorii C. Archives, Przedsiębiorstwo Geologiczne, Wrocław. [In Polish.]

Dunne, L.A. and Hempton, M.R. (1984) Deltaic sedimentation in the Lake Hazar pull-apart basin, southeastern Turkey. *Sedimentology*, *31*, 401–412.

Dyja, E. (1978) Karta otworu wiertniczego Osieczów N-25. National Geological Archives, No. 286163.PIG, Warszawa. [In Polish.].

Elliott, T. (1974) Interdistributary bay sequences and their genesis. *Sedimentology*, *21*, 611–622.

Gani, M.R., Bhattacharya, J.P. and MacEachern, J.A. (2007) Using ichnology to determine relative influence of waves, storms, tides, and rivers in deltaic deposits: examples from Cretaceous Western Interior Seaway, U.S.A. *Society for Sedimentary Geology (SEPM) Short Course Lecture Notes, 52*, pp. 209–227.

Gaynor, G.C. and Swift, D.J.P. (1988) Shannon Sandstone depositional model; sand ridge dynamics on the Campanian Western Interior Shelf. *Journal of Sedimentary Research*, *58*, 868–880.

Gilbert, G.L., O'Neill, H.B., Nemec, W., Thiel, C., Christiansen, H.H. and Buylaer, J.-P. (2018) Late Quaternary sedimentation and permafrost development in a Svalbard fjord-valley, Norwegian high Arctic. *Sedimentology*, *65*, 2531–2558.

Górniak, K. (1986) O sedymentacji santonu niecki północnosudeckiej i możliwości występowania złóż surowców ilastych. *Archiwum Mineralogiczne*, *41*, 123–134. [In Polish with English summary.].

Haq, B.U. (2014) Cretaceous eustasy revisited. *Global and Planetary Change*, *114*, 44–58.

Harms, J.C., Southard, J.B., Spearing, D.R. and Walker, R.G. (1975) Depositional Environments as interpreted from Primary Sedimentary Structures and Stratification Sequences. *Society for Sedimentary Geology (SEPM) Short Course Lecture. Notes, 2*, pp. 161.

Harms, J.C., Southard, J.B. and Walker, R.G. (1982) Structures and Sequences in Clastic Rocks. *Society for Sedimentary Geology (SEPM) Short Course Lecture Notes, 9*, pp. 250.

Hein, F.J. (1987) Tidal/littoral offshore shelf deposits—Lower Cambrian Gog Group, Southern Rocky Mountains, Canada. *Sedimentary Geology*, *52*, 155–182.

Helland-Hansen, W. (2009) Towards the standardization of sequence stratigraphy: discussion. *Earth-Science Reviews*, *94*, 95–97.

Houbolt, J.J.H.C. (1968) Recent sediments in the southern bight of the North Sea. *Geologie en Mijnbouw*, *47*, 245–273.

Howard, J.D. and Reineck, H.E. (1981) Depositional facies of high-energy beach-to-offshore sequence: comparison with low-energy sequence. *AAPG Bulletin*, *65*, 807–830.

Kochanowska, J. (1988) Karta otworu wiertniczego Zebrzydowa-4. Proxima S.A. Report No. DV/2827. Archives, Przedsiębiorstwo Geologiczne, Wrocław. [In Polish.].

Komar, P.D. and Miller, M.C. (1975) The initiation of oscillatory ripple marks and the development of plane-bed at high shear stresses under waves. *Journal of Sedimentary Petrology*, *45*, 697–703.

Krutzsch, W. (1966) Die sporenstratigraphische Gliederung der Oberkreide im nordlichen Mitteleuropa. *Abhandlungen des Zentralen Geologischen Institutes*, *8*, 79–111.

Laprida, C., Chapori, N.G., Violante, R.A. and Compagnucci, R.H. (2007) Mid-Holocene evolution and paleoenvironments of the

shoreface–offshore transition, north-eastern Argentina: New evidence based on benthic microfauna. *Marine Geology*, *240*, 43–56.

Leeder, M.R., Ord, D.M. and Collier, R. (1988) Development of alluvial fans and fan deltas in neotectonic extensional settings: implications for the interpretation of basin-fills. In: Nemec, W. and Steel, R.J. (Eds.) *Fan Deltas—Sedimentology and Tectonic Settings*. London, UK: Blackie, pp. 173–185.

Leszczyński, S. (2010) Coniacian–?Santonian paralic sedimentation in the Rakowice Małe area of the North Sudetic Basin, SW Poland: sedimentary facies, ichnological record and palaeogeographical reconstruction of an evolving marine embayment. *Annales Societatis Geologorum Poloniae*, *80*, 1–24.

Leszczyński, S. (2018) Integrated sedimentological and ichnological study of the Coniacian sedimentation in North Sudetic Basin, SW Poland. *Geological Quarterly*, *62*, 767–816.

Longhitano, S.G. (2013) A facies-based depositional model for ancient and modern, tectonically–confined tidal straits. *Terra Nova*, *25*, 446–452.

Longhitano, S.G. and Nemec, W. (2005) Statistical analysis of bed thickness variation in a Tortonian succession of biocalcarenitic tidal dunes, Amantea Basin, Calabria, southern Italy. *Sedimentary Geology*, *179*, 195–224.

Longhitano, S.G., Chiarella, D. and Muto, F. (2014) Three-dimensional to two-dimensional cross-strata transition in the lower Pleistocene Catanzaro tidal strait transgressive succession (southern Italy). *Sedimentology*, *61*, 2136–2171.

Marciński, J. (1970) Karta otworu wiertniczego Jagodzin 1. National Geological Archives, No. 290731. PIG, Warszawa. [In Polish.].

McBride, R.A. (2003) Offshore sand banks and linear sand ridges. In: Middleton, G.V. (Ed.) *Encyclopedia of Sediments and Sedimentary Rocks*. Dordrecht, Netherlands: Kluiver Academic Publishers, pp. 737–739.

Milewicz, J. (1956) Zaburzenie utworów kredowych w Rakowicach Małych. *Przegląd Geologiczny*, *4*, 361–364. [In Polish.].

Milewicz, J. (1958) Podział stratygraficzny osadów kredowych w niecce północno-sudeckiej. *Przegląd Geologiczny*, *6*, 386–388. [In Polish.].

Milewicz, J. (1965) Facje górnej kredy wschodniej części niecki północnosudeckiej. *Biuletyn Instytutu Geologicznego*, *170*, 15–80. [In Polish.].

Milewicz, J. (1966) Kreda z głębokiego otworu Węgliniec IG1. *Kwartalnik Geologiczny*, *10*, 1144–1146. [In Polish.].

Milewicz, J. (1970) The Cretaceous of the Jerzmanice Graben (Sudetes). *Biuletyn Instytutu Geologicznego*, *239*, 37–66. [In Polish with English summary.].

Milewicz, J. (1973). Niecka północnosudecka. In Sokołowski, S. (Ed.) *Budowa Geologiczna Polski, Tom 1—Stratygrafia, Część 2—Mezozoik*. Warszawa, Poland: Wydawnictwo Geologiczne, pp. 619–628. [In Polish.].

Milewicz, J. (1979) Distribution of cretaceous rocks in the North Sudetic Basin. *Kwartalnik Geologiczny*, *23*, 819–825. [In Polish with English summary.].

Milewicz, J. (1985) A proposal of formal stratigraphic subdivision of the infill of the North Sudetic Depression. *Przegląd Geologiczny*, *33*, 385–389. [In Polish with English summary.].

Milewicz, J. (1991) On development of the North Sudetic Cretaceous Basin. *Biuletyn Państwowego Instytutu Geologicznego*, *367*, 135–141. [In Polish with English summary.].

Milewicz, J. (1997) Upper Cretaceous of the North Sudetic Depression (litho- and biostratigraphy, paleogeography, tectonics and remarks on raw materials). *Acta Universitatis Vratislaviensis, Prace Geologiczno-Mineralogiczne*, *61*, 5–54. [In Polish with English summary.].

Milewicz, J. (1998) Distribution of Coniacian sandstones in the North Sudetic Basin. *Acta Universitatis Vratislaviensis, Prace Geologiczno-Mineralogiczne*, *64*, 101–109. [In Polish with English summary.].

Milewicz, J. (2006) O osadach santońskich na obszarze basenu północnosudeckiego. *Przegląd Geologiczny*, *54*, 693–694. [In Polish.].

Milewicz, J., Podemski, M. and Witwicka, E. (1968) New data on Upper Cretaceous in the western part of the North Sudetic Trough. *Kwartalnik Geologiczny*, *12*, 143–152. [In Polish with English summary.].

Mitchell, A.J., Uličný, D., Hampson, G.J., Allison, P.A., Gorman, G.J., Piggot, M.D. *et al.* (2010) Modelling tidal current-induced bed shear stress and palaeocirculation in an epicontinental seaway: the Bohemian Cretaceous Basin, Central Europe. *Sedimentology*, *57*, 359–388.

Musstow, R. (1968) Beitrag zur Stratigraphie und Paläogeographie der Oberkreide und des Albs in Ostbrandenburg und der östlichen Niederlausitz. *Geologie*, *17*, 1–71.

Nádaskay, R. and Uličný, D. (2014) Genetic stratigraphy of Coniacian deltaic deposits of the northwestern part of the Bohemian Cretaceous Basin. *Zeitschrift der Deutschen Geologischen Gesellschaft*, *165*, 547–575.

Olariu, C., Steel, R.J., Dalrymple, R.W. and Gingras, M.K. (2012) Tidal dunes versus tidal bars: The sedimentological and architectural characteristics of compound dunes in a tidal seaway, the lower Baronia Sandstone (Lower Eocene), Ager Basin, Spain. *Sedimentary Geology*, *279*, 134–155.

Partsch, J. (1896). Schlesien. Eine Landeskunde für das deutsche Volk, 1. Teil: Das ganze Land. Ferdinand Hirt, Breslau.

Perillo, G.M.E. (1995). *Geomorphology and Sedimentology of Estuaries. Developments in Sedimentology, 53*. Amsterdam, Netherlands: Elsevier, pp. 471.

Postma, G. (1990) An analysis of the variation in delta architecture. *Terra Nova*, *2*, 124–130.

Pożaryski, W., Brochwicz-Lewiński, W., Brodowicz, Z., Jaskowiak-Szoenejch, M., Milewicz, J., Sawicki, L. *et al.* (1979) *Geological Map of Poland and Adjoining Countries (without Cenozoic)*. Warszawa, Poland: Wydawnictwo Geologiczne.

Rampino, M.R. and Sanders, J.E. (1981) Evolution of the barrier islands of southern Long Island, New York. *Sedimentology*, *28*, 37–47.

Reineck, H.-E. and Singh, I.B. (1980) *Depositional Sedimentary Environments*. Berlin, Germany: Springer-Verlag, p. 549.

Retallack, G.J. (2001) *Soils of the Past*. Oxford, UK: Blackwell, p. 600.

Reynaud, J.Y., Tessier, B., Proust, J.N., Dalrymple, R., Marsset, T., De Batist, M., *et al.* (1999a) Eustatic and hydrodynamic controls on the architecture of a deep shelf sand bank (Celtic Sea). *Sedimentology*, *46*, 703–721.

Reynaud, J.Y., Tessier, B., Proust, J.N., Dalrymple, R., Bourillet, J.F., De Batist, M., *et al.* (1999b) Architecture and sequence stratigraphy of a late Neogene incised valley at the shelf margin, southern Celtic Sea. *Journal of Sedimentary Research*, *69*, 351–364.

Rossi, V.M., Longhitano, S.G., Mellere, D., Dalrymple, R.W., Steel, R.J., Chiarella, D. and *et al.* (2017) Interplay of tidal and fluvial processes in an early Pleistocene, delta-fed, strait margin (Calabria, Southern Italy). *Marine and Petroleum Geology*, *87*, 14–30.

Sanders, J.E. and Kumar, N. (1975) Evidence of shoreface retreat and in-place "drowning" during Holocene submergence of barriers, shelf off Fire Island, New York. *Geological Society of America Bulletin*, *86*, 65–76.

Scupin, H. (1910) Über sudetische prätertiäre junge Krustenbewegungen und die Verteilung von Wasser und Land zur Kreidezeit in der Umgebung der Sudeten und des Erzgebirges. *Zeitschrift für Naturwissenschaften*, *82*, 321–344.

Scupin, H. (1913) Die Löwenberger Kreide und ihre Fauna. *Palaeontographica-Supplementbőnde*, *6*, 1–276.

Snedden, J.W. and Dalrymple, R.W. (1999). Modem shelf sand ridges: from historical perspective to a unified hydrodynamic and evolutionary model. In Bergman, K.M. and Snedden, J.W. (Eds.) Isolated Shallow Marine Sand Bodies: Sequence Stratigraphic Analysis and Sedimentological Perspectives. *Society for Sedimentary Geology (SEPM) Special Publication, 64*, pp. 13–28.

Swift, D.J.P. (1975) Tidal sand ridges and shoal-retreat massifs. *Marine Geology*, *18*, 105–134.

Taylor, A.M. and Goldring, R. (1993) Description and analysis of bioturbation and ichnofabric. *Journal of the Geological Society (London)*, *150*, 141–148.

Thom, B.G. (1984) Transgressive and regressive stratigraphies of coastal sand barriers in southeast Australia. *Marine Geology*, *56*, 137–158.

Uličný, D., Laurin, J. and Čech, S. (2009) Controls on clastic sequence geometries in a shallow-marine, transtenstional basin: the Bohemian Cretaceous Basin, Czech Republic. *Sedimentology*, *56*, 1077–1114.

Voigt, S., Wagreich, M., Surlyk, F., Walaszczyk, I., Uličny, D. and Čech, S.*et al*. (2008) Cretaceous. In McCann, T. (Ed.) *The Geology of Central Europe, 2. Mesozoic and Cenozoic*. London, UK: Geological Society, pp. 923–998.

Walaszczyk, I. (2008) North Sudetic Basin (Outer Sudetic Cretaceous). In McCann, T. (Ed.) *The Geology of Central Europe, 2 (Mesozoic and Cenozoic)*. London, UK: Geological Society, pp. 959–960.

Walker, R.G. (1984). General introduction: facies, facies sequences and facies models. In Walker, R.G. (Ed.) Facies Models, 2nd edition. *Geoscience Canada Reprint Series, 1*, pp. 1–9.

Williger, G. (1882) Die Löwenberger Kreidemulde, mit besonderer Berücksichtigung ihrer Fortsetzung in der preussischen Ober-Lausitz. *Jahrbuch der königlichen preussischen geologischen Landesanstalt*, *1882*, 55–125.

Wood, M.L. and Ethridge, F.G. (1988) Sedimentology and architecture of Gilbert- and mouth bar-type fan deltas, Paradox Basin, Colorado. In: Nemec, W. and Steel, R.J. (Eds.) *Fan Deltas—Sedimentology and Tectonic Settings*. London, UK: Blackie, pp. 251–263.

Wright, L.D. (1977) Sediment transport and deposition at river mouths: a synthesis. *Geological Society of America Bulletin*, *88*, 857–868.

Żelaźniewicz, A., Aleksandrowski, P., Buła, Z., Karnkowski, P.H., Konon, A., Oszczypko, N.*et al*. (2011). Regionalizacja Geologiczna Polski. Komitet Nauk Geologicznych Polskiej Akademii Nauk, Wrocław, pp. 60. [In Polish.].

Ziegler, P.A. (1990) *Geological Atlas of Western and Central Europe*, 2nd edition. Amsterdam, Netherlands: Shell Publication, Elsevier.

How to cite this article: Leszczyński S, Nemec W. Sedimentation in a synclinal shallow-marine embayment: Coniacian of the North Sudetic Synclinorium, SW Poland. *Depositional Rec*. 2020;6:144–171. https://doi.org/10.1002/dep2.92